

THE REDSHIFT-SPACE TWO-POINT CORRELATION
FUNCTIONS OF GALAXIES AND GROUPS IN THE
NEARBY OPTICAL GALAXY SAMPLE

Giuliano GIURICIN^{1,2}, Srdjan SAMUROVIC^{1,3}, Marisa GIRARDI¹,

Marino MEZZETTI¹, Christian MARINONI¹

¹ Dipartimento di Astronomia, Univ. di Trieste, via G.B. Tiepolo 11, 34131 Trieste, Italy

² SISSA, via Beirut 4, 34013 Trieste, Italy

³ International Center for Theoretical Physics, Strada Costiera 11, 34014 Trieste, Italy

E-mail: giuricin@sissa.it, srdjan@tsastro.it, girardi@tsastro.it

mezzetti@tsastro.it, marinoni@sissa.it

Received _____; accepted _____

A B S T R A C T

We use the two-point correlation function in redshift space, $\xi(s)$, to study the clustering of the galaxies and groups of the Nearby Optical Galaxy (NOG) sample, which is a nearly all-sky ($b_j > 20^\circ$), complete, magnitude-limited sample of 7000 bright and nearby optical galaxies ($cz \leq 6000$ km/s).

The correlation function of galaxies is well described by a power law, $\xi(s) = (s=s_0)^{-\gamma}$, with slope $\gamma = 1.5$ and $s_0 = 6.4 h^{-1} \text{Mpc}$ (on scales $2.7 \leq s \leq 12 h^{-1} \text{Mpc}$), in substantial agreement with previous results of several redshift surveys of optical galaxies.

Splitting NOG into different morphological subsamples, we confirm the existence of morphological segregation between early- and late-type galaxies (out to $20 h^{-1} \text{Mpc}$) and, in particular, we find a gradual decreasing of the strength of clustering from the S0 galaxies to the late-type spirals, on intermediate scales (around $5 h^{-1} \text{Mpc}$). The relative bias factor between early- and late-type galaxies appears to be substantially constant with scale.

Furthermore, luminous galaxies turn out to be more clustered than dim galaxies. The luminosity segregation, which is significant for both early- and late-type objects, starts to become appreciable only for galaxies brighter than $M_B = -19.5 + 5 \log h$ ($0.6 L$) and is independent on scale.

The NOG groups identified with the hierarchical and percolation algorithms show similar clustering properties, with a degree of clustering which is intermediate between galaxies and clusters. The group correlation functions are characterized by s_0 -values ranging from $8 h^{-1} \text{Mpc}$ (for groups with at least three members) to $10 h^{-1} \text{Mpc}$ (for groups with at least five members). The degree of group clustering depends on the physical properties of groups. Specifically, groups with greater velocity dispersions, sizes and masses tend to

{ 3 {

be more clustered than those with lower values of these quantities.

Subject headings: galaxies: clusters: general - cosmology: large-scale structure
of universe

1. Introduction

The two-point correlation function (hereafter CF) has been the first and most widely used approach to quantify the degree of clustering in a galaxy sample (Totsuji & Kihara 1969; Peebles 1980). This statistics has been widely applied to a variety of samples of optically- and infrared-selected galaxies, groups and clusters of galaxies. Besides, it has been used to characterize the dependence of the galaxy clustering on the internal properties of galaxies such as morphology (e.g., Davis & Geller 1976), color (e.g., Tucker et al. 1995), surface brightness (Davis & Djorgovski 1985), luminosity (e.g., Maurogordato & Lachieze-Rey 1987), and internal dynamics (e.g., White, Tully, & Davis 1988).

From galaxies to clusters the CF in redshift space, $\xi(s)$, is characterized by a power-law form, $\xi(s) = (s/s_0)^{-\gamma}$, with $1.5 \leq \gamma \leq 2$ for a variety of systems. The correlation length s_0 ranges from $5 \leq 7.5 h^{-1} \text{ Mpc}$ for optically-selected galaxies (e.g., Wilmer, da Costa, & Pellegrini 1998 and references cited therein) to $s_0 > 15 h^{-1} \text{ Mpc}$ for optically- and X-ray selected galaxy clusters (e.g., Bahcall & Soneira 1983; Postman, Huchra, & Geller 1991; Peacock & West 1992; Croft et al. 1997; Borgani, Plionis, & Kolokotronis 1999). (Throughout, the Hubble constant is $H_0 = 100 h \text{ km s}^{-1} \text{ Mpc}^{-1}$).

Results are far less clear for loose galaxy groups. Jing & Zhang (1988) and Maia & da Costa (1989) calculated the CF of the groups identified in the CfA1 and SSRS redshift surveys and found that the amplitude of the group CF is lower than that of the galaxy CF. Later, from the analysis of the groups identified in a subsample of the CfA2 redshift survey, Ramella, Geller, & Huchra (1990) found that the amplitudes of the two CFs were similar (see also Kalinkov & Kuneva 1990). Recently, Trasarti-Battistoni, Invernizzi, & Bonometto (1997), who analyzed groups identified in the Perseus-Pisces region, and Girardi, Boschini, & da Costa (2000), who considered the groups respectively identified by Ramella, Pisani, & Geller (1997) and Ramella et al. (2000) in the CfA2 and SSRS2 redshift surveys, stressed

that groups are more clustered than galaxies.

In this paper we determine the CF (in redshift space) of the galaxies and groups in the nearby universe, by using the NOG ("Nearby Optical Galaxies") sample (Giuricin et al. 2000), which is a complete, distance-limited ($cz \leq 6000$ km/s) and magnitude-limited sample of 7000 nearby and bright optical galaxies, which covers $\Omega = 3$ of the sky (8.27 sr).

This paper is the fourth in a series of papers, in which we investigate on the properties of the large-scale galaxy distribution in the nearby universe by using a nearly all-sky sample of optical galaxies (Marinoni et al. 1998, Paper I; Marinoni et al. 1999, Paper II; Giuricin et al. 2000, Paper III). In a forthcoming paper (Marinoni, Hudson, & Giuricin 2001) the optical luminosity function of all galactic systems derived from the NOG will be compared to theoretical predictions of the mass function of virialized haloes.

The NOG is currently one of the largest samples used in the determination of the galaxy CF, and, compared to other wide-angle, comparatively shallow, bright magnitude-limited galaxy samples, such as the CfA1, CfA2, and SSRS2 redshift surveys, the NOG may be less sensitive to local density fluctuations because it covers a much larger solid angle.

Besides comparing our results with those obtained from other galaxy samples, with our wide sample we examine the dependence of the correlation properties of galaxies on galaxy morphology, attempting a subdivision of galaxies in several morphological subtypes.

We also investigate on the dependence of the galaxy CF on galaxy luminosity. In this respect our analysis differs from previous relevant studies because we rely on blue total magnitudes fully corrected for internal extinction, Galactic extinction, and K-dimming. These corrections lead to brighter magnitudes. In particular the first correction, which is conspicuous in very inclined spirals, is generally neglected in generic redshift surveys, which comprise many faint galaxies of unknown inclination. Some authors (e.g. Hasegawa

& Umemura 1993) have contended that this correction has a non negligible impact on the determination of luminosity segregation.

Furthermore, we investigate on the dependence of the group CF on group properties, relying on two catalogs of groups identified with the hierarchical and percolation friends of friends algorithms. Being extracted from the same galaxy sample, these catalogs allow us to investigate, for the first time, on possible differences in clustering properties strictly related to differences in the algorithm adopted. In the literature there are as yet no studies dealing with the CF of groups identified with the hierarchical algorithm.

The outline of our paper is as follows. In §2 we briefly describe the NOG samples of galaxies and groups used in this study. In §3 we deal with the estimate of the redshift-space CF. In §4 we present the CF of the NOG galaxies. In §5 and §6 we examine the dependence of the galaxy CF on galaxy morphology and luminosity, respectively. In §7 we present the CF of the NOG groups and compare it with that of galaxies in order to determine the relative clustering properties. In §8 we explore the dependence of the group CF on group properties (e.g., on velocity dispersions, radii, and masses). Conclusions are drawn in §9.

2. The Samples of Galaxies and Groups

In this work we use the NOG sample of galaxies (described in Paper III) basically extracted from the Lyon-Meudon Extragalactic Database (LED A; e.g. Paturel et al. 1997) according to the following selection criteria: i) galactic latitudes $|b| > 20^\circ$; ii) recession velocities (evaluated in the Local Group rest frame) $cz < 6000$ km/s; iii) corrected total blue magnitudes $B - 1.4$ mag. In the LED A compilation, which collected and homogenized several data for all the galaxies of the main optical catalogs, the original raw data (blue apparent magnitudes and angular sizes) have been transformed to the standard systems

of the RC3 catalog (de Vaucouleurs et al. 1991) and have been corrected for Galactic extinction, internal extinction, and K -dimming. The degree of the redshift completeness of the NOG is estimated to be 97% . In this work we consider the sample of 7028 galaxies having $cz \leq 50$ km /s.

Almost all NOG galaxies (98.7%) have a morphological classification. We divide NOG galaxies into two broad morphological bins, early-type galaxies, i.e. E-S0 galaxies ($T < 1.5$) and late-type galaxies ($T \geq 1.5$), hereafter denoted as Sp, which comprise S0/a galaxies and later types (T is the morphological type code system of the RC3 catalog). We also attempt a finer morphological subdivision, dividing galaxies into 6 morphological bins, E ($T < 2.5$), S0 ($2.5 \leq T < 1.5$), S0/a ($1.5 \leq T < 0.5$), Sa ($0.5 \leq T < 2.5$), Sb ($2.5 \leq T < 3.5$), and later types (Sc+ Sd+ Sm + Irr, i.e. $T \geq 3.5$, hereafter simply denoted as Scd). The first subsample, hereafter denoted by E for the sake of simplicity, does not comprise only ellipticals but also lenticulars, since it contains also objects broadly classified as E-S0.

We also use the catalogs of NOG groups identified within the NOG by means of the hierarchical (H) and the percolation (P) algorithms (see Paper III).

In the H method the authors adopted the galaxy luminosity density as the affinity parameter used to construct the dendrogram and cut the hierarchy at a luminosity density corresponding to a luminosity density contrast of 45 in order to identify groups. In order to take into account the decrease of the magnitude range of the luminosity function sampled at increasing distance, the galaxy luminosities were suitably increased with distance.

The authors employed two variants of the P method to identify groups. In the first variant the authors adopted a velocity link parameter of $cz = 200$ km /s and a distance link parameter of $0.31 h^{-1}$ Mpc at the fiducial velocity of 500 km /s (the latter value corresponds to a number density threshold of 80). Both link parameters were then suitably scaled

with distance. In the second variant the authors scaled with distance only the distance link parameter and kept the velocity link parameter constant at the value of 350 km/s. Given the limited range of redshift encompassed by the NOG, this choice was used as an approximation to a slow scaling of cz with distance, which was suggested by several cosmological N -body simulations (e.g., Nolthenius & White 1987; see Paper III for details on group identifications).

Excluding the Local Group, in this paper we consider the 474 groups with at least three members (of which 61 have at least ten members) obtained with the H method (H groups) and the 506 groups with at least three members (of which 62 have at least ten members) obtained with the second variant of the P method (P groups). About 45% of the NOG galaxies are found to be group members. For the sake of simplicity, in this paper we do not consider groups obtained with the first variant of the P method, because the two variants gave very similar catalogs of groups.

The catalogs of NOG groups are among the largest catalogs of groups presently available in the literature. Being extracted from the same galaxy sample, the catalogs of H and P groups allow us also to investigate on differences in the group clustering properties related to differences in the algorithm of group identification.

For the analyses presented in this paper, we construct volume-limited subsamples, which by definition contain objects that are luminous enough to be included in the sample when placed at the cutoff distance.

Basically, we define volume-limited subsamples of galaxies with depth of 3000, 4000, 5000, and 6000 km/s. They contain 1615, 1895, 2220, and 2257 galaxies, respectively. The absolute magnitude limits corresponding to these distances are $M_B = -18.39, -19.01, -19.49,$ and -19.89 mag, respectively (here and throughout this paper, in general we omit the 5 log h term in the absolute magnitude).

Moreover, we construct volume-limited samples of H and P groups with depth of 4000 km/s, by using suitably modified versions of the H and P algorithms in which the selection parameters which scale with distance are kept fixed at the values corresponding to 4000 km/s. These volume-limited samples contain 140 H and 141 P groups (with $n = 3$ members).

3. Calculating the Two-Point Correlation Function

We define the separation in redshift space, s , as

$$s = H_0^{-1} \sqrt{V_i^2 + V_j^2 - 2V_i V_j \cos \theta_{ij}} \quad (1)$$

where V_i and V_j are the velocities of two objects (galaxies or groups) separated by an angle θ_{ij} on the sky. We calculate the CF in redshift space, $\xi(s)$, using the estimator proposed by Hamilton (1993)

$$\xi(s) = \frac{DD(s)RR(s)}{[DR(s)]^2} - 1 \quad (2)$$

where $DD(s)$, $RR(s)$, and $DR(s)$ are the number of data{data, random {random, and data{random pairs, respectively, with separation in the interval $(s - ds, s + ds)$. Compared to the classical estimator of $\xi(s)$ by Davis & Peebles (1983), which explicitly depends on the mean density assigned to the sample, Hamilton's estimator is less affected by the uncertainty in the mean density, which is only a second-order effect. In particular, numerical simulations have shown that Hamilton's estimator performs better on large scales where the clustering is weak (see, e.g., Pons-Borderia et al. 1999 and Kerscher, Szapudi, & Szalay 2000) for a thorough comparison of the reliability of several estimators of CF). We generate the random sample by filling the sample volume with a random distribution

of the same number of points as in the data. The random points are distributed in depth according to the selection function of the data sample.

In order to minimize the statistical fluctuations in the determination of CF, we average the results obtained using many different replicas of the random sample. In general we compute 50 replicas in the case of galaxies and 400 in the case of groups.

The counts $DD(s)$, $DR(s)$, and $RR(s)$ can be generalized to include a weight w , which is particularly important to correct for selection effects at large distances in a magnitude-limited samples. As a matter of fact, magnitude-limited samples become sparser at larger distances due to the increasing loss of galaxies caused by the apparent magnitude cut-off. This effect is quantified by the selection function $S(s)$, which expresses the fraction of objects that are expected to satisfy the sample's selection criteria. For $s < s_*$, where s_* is a fiducial distance that we take to be equal to $500 \text{ km s}^{-1} = H_0 = 5 h^{-1} \text{ Mpc}$, the appropriate selection function for a magnitude-limited sample is simply $S(s) = f$, where f is the average completeness level of the sample ($f = 0.97$ for the NOG), whereas for $s > s_*$ the selection function is

$$S(s) = f \frac{\int_{L_s}^{L_{\max}} L_{\min}(s) (L) dL}{\int_{L_s}^{L_{\max}} (L) dL} \quad (3)$$

where L is the luminosity function, $L_{\min}(s)$ is the minimum luminosity necessary for a galaxy at a distance s (in Mpc) to make it into the sample and the integral is cut-off at the lower limit of $L_s = L_{\min}(s)$. $L_{\min}(s)$ corresponds to the absolute magnitude $M_B = -5 \log s - 25 + B_{\lim}$, where $B_{\lim} = 14 \text{ mag}$ is the limiting apparent magnitude of NOG; thus L_s corresponds to the absolute magnitude $M_s = -14.50 \text{ mag}$.

In the calculation of the selection function we use the Schechter (1976) form of the luminosity function that we derive by means of Turner's (1979) method (see also de

Lapparent, Geller, & Huchra 1989, and Paper II), using redshifts as distance indicators, for the whole sample and for specific morphological subsamples. The adopted Schechter parameters are $\alpha = -1.2$ and $M_B = -20.0$ (see Paper III) for the whole NOG (see also paper II for the values appropriate for the specific morphological types). We have checked that our results on CFs are insensitive to changes of M and α by 0.2 mag and 0.1, respectively.

Unless otherwise specified, we compute the weighted CF by replacing the counts of pairs with the weighted sum of pairs, $\sum_i^P w_i w_j$, which takes into account the selection effects acting on the sample used. The weighting scheme we adopt is that of equally weighted volumes, $w_i = 1/S(s_i)$, where $S(s)$ is the selection function. We do not use the minimum variance weighting scheme (Davis & Huchra 1982), which requires prior knowledge of the CF. However, for a dense sample like the NOG, the practical improvement provided by using the minimum variance method is very small (Hamilton 1993; Park et al. 1994).

In several cases we use volume-limited subsamples. This is equivalent to applying a lower limit to the luminosity of the objects of the subsample, leading to a uniformly selected data set with the same weight assigned to each object ($S(s) = f; 0 \leq s \leq s_{\max}$).

We calculate the errors for the $\xi(s)$ by using 100 bootstrap resamplings of the data (e.g., Ling, Frenk, & Barrow 1986); bootstrapping tends to overestimate the real errors, as shown by Fisher et al. (1994).

Since in general $\xi(s)$ is satisfactorily described by a power law over a fairly large interval of s , we always fit $\xi(s)$ to the form $\xi(s) = (s/s_0)^{\gamma}$ with a non-linear weighted least-squares method in the intervals where $\xi(s)$ is reasonably fitted by a single power-law. Since the points are not statistically independent, it is not strictly correct to use a least-squares method for doing the fit. But it is a satisfactory approximation (Bouchet et al. 1993) especially if we bear in mind that in any case the results of the power-law fits are sensitive

to the interval adopted in the fits. Besides, the underestimation of the fit errors due to the bin-bin interdependence is well compensated by the overestimation given by the bootstrapping-resampling method (Mo, Jing, & Bomer 1992).

The variance of galaxy counts in the volume V is related to the moment of $\xi(s)$ which gives the separation {averaged value of $\xi(s)$ in the volume V ,

$$\sigma^2 = \frac{1}{V^2} \int_V \int_V dV_1 dV_2 \langle \xi(\mathbf{r}_1 - \mathbf{r}_2) \rangle \quad (4)$$

For a power-law correlation function $\xi(s) = (s/s_0)^{\gamma}$ and a spherical radius of radius R , this integral can be performed analytically to yield (cf. Peebles 1980, section 59.3)

$$\sigma^2(R) = \frac{72 (s_0/R)^{\gamma}}{2(3-\gamma)(4-\gamma)(6-\gamma)} \quad (5)$$

We use this expression to calculate the rms fluctuation in galaxy counts within a sphere of $8 h^{-1} \text{ Mpc}$ radius, r_8 , a quantity which is often used to normalize theoretical models.

We evaluate the relative bias between two samples of galaxies of different luminosities or morphological types through the expression

$$\frac{b}{b}^*(s) = \frac{\overline{\xi}^*(s)}{\overline{\xi}(s)} \quad (6)$$

where the starred symbols denote a sample taken as a fiducial.

4. The correlation function of NOG galaxies

4.1. Results for the whole NOG

The redshift-space weighted CF from the whole NOG sample, (7028 galaxies in the velocity range $50 < cz < 6000 \text{ km/s}$) is satisfactorily described by a power law in the

interval $1 < s < 15 h^{-1} \text{ Mpc}$. Error bars become progressively larger beyond $10 h^{-1} \text{ Mpc}$.

From a power-law fit calculated in the interval $2.7 - 12 h^{-1} \text{ Mpc}$, which in this case and in most subsamples of galaxies examined in this paper is the one where $\xi(s)$ is best-fitted by a single power law, we obtain a correlation length of $s_0 = 6.42 \pm 0.11 h^{-1} \text{ Mpc}$ and a slope $\gamma = 1.46 \pm 0.05$. From these values we estimate a value of $\xi_8 = 1.03 \pm 0.02$.

More specifically, $\xi(s)$ is not a perfect power-law. It tends to flatten on small scales ($s < 2 h^{-1} \text{ Mpc}$) because of the effects of peculiar motions, which smear out galaxy systems along the radial line-of-sight. It tends to steepen on large scales ($s > 15 h^{-1} \text{ Mpc}$). For instance, we find $s_0 = 6.12 \pm 0.10 h^{-1} \text{ Mpc}$, $\gamma = 1.39 \pm 0.03$ in the range $1.1 \leq s \leq 17 h^{-1} \text{ Mpc}$, and $s_0 = 6.24 \pm 0.09 h^{-1} \text{ Mpc}$, $\gamma = 1.58 \pm 0.05$ in the range $2.7 \leq s \leq 17 h^{-1} \text{ Mpc}$.

Our values of s_0 and γ turn out to be in good agreement with those relative to the redshift-space $\xi(s)$ derived from the SSRS1 sample (Maurogordato, Schaefer, & da Costa 1992; $s_0 = 5.8 \pm 0.5 h^{-1} \text{ Mpc}$, $\gamma = 1.6$), SSRS2 sample (Wilmer et al. 1998; $s_0 = 5.85 \pm 0.13 h^{-1} \text{ Mpc}$, $\gamma = 1.60 \pm 0.08$), the sparsely sampled Stromlo-APM survey (Loveday et al. 1995; $s_0 = 5.9 \pm 0.3 h^{-1} \text{ Mpc}$, $\gamma = 1.47 \pm 0.12$), the Las Campanas Redshift Survey (LCRS; Tucker et al. 1997; $s_0 = 6.28 \pm 0.27 h^{-1} \text{ Mpc}$; $\gamma = 1.52 \pm 0.03$).

Besides, the amplitude of the NOG $\xi(s)$ is consistent with that of the Optical Redshift Survey (ORS; Hemit et al. 1996; $s_0 = 6.6 \pm 0.8 h^{-1} \text{ Mpc}$, $\gamma = 1.57; 1.51$ for the ORSd and ORSm samples, respectively) and that of the CfA2 survey (de Lapparent, Geller, & Huchra 1988) ($s_0 = 7.5 \pm 1.7 h^{-1} \text{ Mpc}$, $\gamma = 1.6 \pm 0.1$), which encompasses the Great Wall, an overdense region characterized by a very high degree of local clustering ($s_0 \sim 15 h^{-1} \text{ Mpc}$, see Ramella, Geller, & Huchra 1992).

In Figure 1 we compare the redshift-space galaxy CF from the whole NOG with the redshift-space galaxy CFs from some recent redshift surveys, i.e. the Stromlo-APM

(Loveday et al. 1995), LCRS (Tucker et al. 1997), Durham-UKST (Ratcliffe et al. 1996), and EPS (Guzzo et al. 2000) redshift surveys.

Our results are in good agreement with the results from Stromlo-APM and especially with those from LCRS, although the volumes of the last two surveys ($2.5 \times 10^3 \text{ h}^{-3} \text{ Mpc}^3$ and $2.6 \times 10^3 \text{ h}^{-3} \text{ Mpc}^3$, respectively) are quite larger than that of NOG ($5.95 \times 10^3 \text{ h}^{-3} \text{ Mpc}^3$). On small scales ($s < 6 \text{ h}^{-1} \text{ Mpc}$), our results also agree with those from the sparsely-sampled Durham-UKST survey (encompassing a volume of $4 \times 10^3 \text{ h}^{-3} \text{ Mpc}^3$), which, however, around $s \sim 10 \text{ h}^{-1} \text{ Mpc}$, leads to a $\xi(s)$ characterized by a somewhat large amplitude. On the other hand, the amplitude of the NOG $\xi(s)$ is slightly larger than that of the ESP sample (characterized by $s_0 \sim 5 \text{ h}^{-1} \text{ Mpc}$, $\xi(s) \sim 1.5$), which, owing to its faint magnitude limit, probably contains a much larger population of intrinsically faint, less clustered galaxies.

Noticeably, we obtain a smoother $\xi(s)$ than do several previous works probing larger volumes (see, e.g. the results from the Stromlo-APM and Durham-UKST surveys plotted in Figure 1) because NOG contains a large number of galaxies.

4.2. Results for different subsamples

An important issue to test is the reliability of the weights assigned to each galaxy. We do that by comparing magnitude-limited subsamples truncated at a given maximum distance cz_{max} to their volume-limited counterparts. The magnitude- and volume-limited subsamples probe the same volume in space and therefore should lead to the same CF, if the weight in the magnitude-limited subsamples are unbiased, unless there is a strong dependence of clustering on luminosity.

Results of this test are presented in Figures 2 and 3. Figure 2 shows the weighted and

unweighted CFs of the whole NOG sample (7028 galaxies) and the volume-limited sample limited at 6000 km/s (2257 galaxies). Analogously, Figure 3 shows the comparison between the CF of the magnitude-limited (4364 galaxies) and volume-limited (1895 galaxies) subsamples limited at 4000 km/s.

In Figures 2 and 3 the CFs of the volume-limited samples satisfactorily agree with the weighted CFs of the magnitude-limited samples. This reassures of the validity of the selection function adopted for the NOG. On the other hand, the unweighted CFs have markedly smaller amplitudes. The differences between the results of the two weighting schemes (in this case as well as in other cases mentioned below) stem from the fact that the weighted CF weights each volume of space equally and therefore traces better the clustering of more distant and luminous objects, whereas the unweighted CF is more sensitive to the clustering of nearer and fainter objects. In general, throughout this paper we find that the amplitudes of the weighted CFs are significantly larger than those of their unweighted counterparts and that magnitude-limited and volume-limited subsamples restricted to smaller depths have CFs of smaller amplitudes with respect to subsamples of greater depths. (cf. the CFs of Figures 2 and 3). The latter effects are apparent also in several previous works (e.g. Hermít et al. 1996; Wilmer et al. 1998).

Both pronounced tendencies are at least partially due to an increasing clustering with luminosity (we discuss this issue in §6). This effect also explains why indeed the volume-limited sample with depth of 6000 km/s tends to lead to a slightly greater CF than the corresponding magnitude-limited sample (see Figure 2).

There are appreciable variations in CFs among small subsamples of NOG. For instance, we have checked that the CF of the subsample (out to 6000 km/s) relative to the strip of the sky between the UGC and ESO galaxy catalogs ($17^{\circ}5' - 2^{\circ}5'$) is characterized by an appreciably smaller amplitude and a steeper slope than that of the whole sample, from

which the CFs of the regions covered by UGC and ESO (i.e. > 2.5 and < 17.5 , respectively) do not appreciably depart. Thus, we confirm the results by Hermít et al. (1996), who, relying on the diameter-limited ORS sample, noted the peculiar clustering properties of the above-mentioned strip in the nearby universe.

5. Morphological Segregation

We analyze the dependence of clustering on galaxy morphology, calculating the CFs for different morphological types. Studies of morphological segregation based on the comparison of two-point correlation functions are complementary to analyses which deal with the relation between galaxy morphology and local galaxy number density, the morphology-density relation. This relation was defined by Dressler (1980) for galaxy clusters and most of relevant analyses refer to cluster regions, i.e., to scales smaller than

$1.5 h^{-1} \text{ Mpc}$ (see, e.g., Andreon, Davoust, & Heim 1997 and Dressler et al. 1997 for recent accounts of the morphology-density relation). But it was soon suggested that this relation extends outside clusters, i.e. in groups (e.g., Bhavsar 1981, de Souza et al. 1983) and in the field (Postman & Geller 1984). Investigations on morphological segregation have also exploited other statistical descriptors of galaxy clustering (e.g., Lahav & Saslaw 1992; Domínguez-Tenreiro et al. 1994).

Figure 4 shows the weighted CFs for the E-S0 and Sp objects of the whole sample and the magnitude-limited sample out to 4000 km/s . For these magnitude-limited samples and for all volume-limited samples considered, E-S0 galaxies are always more clustered than spirals out to large scales ($> 20 h^{-1} \text{ Mpc}$). Thus we confirm the results of many previous works on the morphological segregation between early- and late-type galaxies (e.g., the early works by Davis & Geller 1976; Giovanelli, Haynes, & Chincarini 1986; Iovino et al. 1993).

Remarkably, analyzing the volume-limited sample with depth of 3000 km/s, we find that an appreciable morphological segregation between early- and late-type galaxies is present also at relatively low luminosities (i.e., at $M_B > -19$ mag), in spite of some recent doubts expressed by Beisbart & Kerschner (2000) who claimed that this morphological segregation concerns essentially luminous galaxies. Thus, our results support the contention (e.g., the review by Ferguson & Binggeli 1994) that the well-known morphology-density relation inferred for the classical Hubble morphological types (Dressler 1980) holds also for dwarf galaxies.

We also attempt to use a fine morphological subdivision. Figures 5 and 6 show the weighted CFs for 6 morphological types, E, S0, S0/a, Sa, Sb, and Scd (see x2 for details on the adopted morphological subdivision) for the whole NOG sample.

Table 1 reports the power-law fit parameters for the various morphological types. These calculations refer to the interval of separations (mostly the 2:7 s 12 h⁻¹ Mpc range) where the CF is in general well approximated by a power law.

If we had attempted to subdivide the E galaxies into two subtypes (i.e., $T < 3.5$ and $3.5 \leq T < 2.5$) we would have found two indistinguishable CFs for the appropriate selection functions. Analogously, if we had subdivided the Sa galaxies into two subtypes (i.e., $0.5 \leq T < 1.5$ and $1.5 \leq T < 2.5$) we would have obtained two indistinguishable CFs for the appropriate selection functions.

Using the whole magnitude-limited sample is an attempt to extract the maximum signal from the available data, but can have some drawbacks in the presence of luminosity segregation (see x6), if the type-specific luminosity functions are not similar. In particular, it is known that Scd galaxies are typically less luminous than the other types (see, e.g., Paper II). Therefore, we have considered also the morphological subsamples extracted from the volume-limited sample at 6000 km/s. Table 2 reports the power-law fit parameters for

these subsamples, except for the 101 S0/a galaxies, whose CF is very noisy and can not be reasonably approximated by a power law.

Figures 5 and 6 and Tables 1 and 2 show that, in general, also morphological subtypes exhibit an appreciable morphological segregation. In general, especially at intermediate scales (around $5 h^{-1} \text{Mpc}$) there appears to be a gradual decreasing of the strength of clustering from the early-types, specially from S0 galaxies, to the latest types, the Scd galaxies. In several cases the morphological segregation between the various types persists out to large scales ($\sim 15 h^{-1} \text{Mpc}$). As regards the E galaxies, these objects do not exhibit a greater clustering than the S0s. Remarkably, if we had subdivided the E-S0 objects into earlier and later types choosing a different limit in T , i.e. $T < 3.5$ and $T \geq 3.5$, we would have found again that the earlier types do not cluster more strongly than the later ones.

The relative differences in the clustering of the various morphological types are confirmed by the analysis of other magnitude-limited samples and volume-limited samples (e.g., the samples truncated at 4000 km/s). Besides, our results on s_0 do not change much if we calculate power-law fits keeping fixed at the value of 1.5, which is typical for the CF of the whole NOG.

A comparison between Table 1 and 2 reveals that, for all morphological subtypes, the CFs derived from volume-limited samples tend to have greater amplitudes than those derived from the corresponding magnitude-limited samples, which is likely to be an effect of luminosity segregation (see x6). Besides, at least partly for the same reason, morphological subsamples limited to smaller depths tend to have CFs of lower amplitudes, as in the general case (see x4.2).

Although the statistical significance of the morphological segregation can be based on the values of the fit parameters (together with associated errors) reported in Tables 1 and

2, it is useful to provide a further check on this effect. For example, we have decided to test the significance of the difference between the CF amplitudes of the volume-limited samples (at the depth of 6000 km/s) of the E-S0 and Sp objects, whose s_0 -values are different at the 6% confidence level. We have addressed this point by randomly selecting two sets of objects of sizes equal to the sizes of the two volume-limited samples from which they are extracted. We have compared the two resulting CFs, which are typically similar. For 500 random selections, the mean ratios between the CF amplitudes are always smaller than the observed value (2.5 in the usual s -range) for the two volume-limited samples. This implies that the two CFs are different at the $> 99.8\%$ confidence level.

Our s_0 -value for the E-S0 objects better agrees with the high values of s_0 reported for the early-type galaxies of the Stromlo-APM and Perseus(Pisces samples (i.e. $s_0 = 9.6 \pm 0.2 \text{ h}^{-1} \text{ Mpc}$ in the redshift space and $s_0 = 8.4 \pm 0.3 \text{ h}^{-1} \text{ Mpc}$ in the real space; see Loveday et al. 1995 and Guzzo et al. 1997, respectively) than with the relatively low values of s_0 ($s_0 = 6 \pm 0.7 \text{ h}^{-1} \text{ Mpc}$) reported for the early-type objects of the SSR S1, (Santiago & Da Costa 1990), ORS (Hernit et al. 1996) and SSR S2 (Wilmer et al. 1998) surveys.

On the other hand, our s_0 -value for Sp galaxies appears to be in substantial agreement with several relevant previous results ($s_0 = 5.3 \pm 0.4 \text{ h}^{-1} \text{ Mpc}$ according to Loveday et al. 1995 and Wilmer et al. 1998), whereas it is somewhat greater than the value ($s_0 = 4.5 \text{ h}^{-1} \text{ Mpc}$) reported by Santiago & Da Costa (1990) for the SSR S1 sample. Hernit et al. (1996) subdivided the ORS spirals into Sab and Scd types. The s_0 -values reported by the authors for these two types are in substantial agreement with the values we obtain for the Sb and the Scd types, respectively.

The lower amplitude of the CF of the IRAS 1.2 Jy redshift survey (Fisher et al. 1994) ($s_0 = 4.53 \pm 0.22 \text{ h}^{-1} \text{ Mpc}$, $\beta = 1.28 \pm 0.04$) compared with that of NOG and many other optical samples, for all galaxies and for all spirals, reflects the relative bias that exists

between optical- and infrared-selected galaxies. The CF amplitude of the NOG Scd galaxies approaches that of the IRAS samples (see also Seaborn et al. 1999 and Szapudi et al. 2000 for the CF of the PSCz sample).

Figure 7 shows the relative bias (b_1/b_2) between the E-S0 and Sp objects (see eq. 6) of the whole NOG as a function of the scale for the whole NOG. This bias appears to be substantially constant with scale. The relative bias (b_1/b_2) between the E-S0 and Scd objects turns out to be also constant with scale. These results are confirmed by the inspection of magnitude-limited and volume-limited samples with smaller depths. We have verified that also the relative biases between other morphological types appear to be substantially constant with scale at least up to $10 h^{-1} \text{Mpc}$. As a matter of fact, all fitting values of b relative to the various morphological types appear to be substantially not inconsistent with the value of $b = 1.5$ which pertains to the whole NOG sample. In other words, there is no sure evidence for an increasing or decreasing value of b as we go from early to late types.

Our results disagree with those by Wilmer et al. 1998 (confirmed by the reanalysis of Beisbart & Kerscher 2000), who found that the relative bias between the SSRS2 E-S0 and Sp (calculated from both redshift-space and real-space correlation functions) decreases from small ($1 h^{-1} \text{Mpc}$) to relatively large ($8 h^{-1} \text{Mpc}$) scales. Also Guzzo et al. (1997) reported a similar scale-dependent bias in their real-space correlation function analysis of the Perseus-Pisces region. Hermitt et al. (1996) claimed a similar effect (in redshift space) for the early-type and late-type ORS objects in the $1 - 10 h^{-1} \text{Mpc}$ range. But the bias appears to grow with scale from $10 h^{-1} \text{Mpc}$ to $20 h^{-1} \text{Mpc}$ so that on large scales ($20 h^{-1} \text{Mpc}$) it is not substantially different from the value relative to small scales ($1 h^{-1} \text{Mpc}$). Furthermore, there is no clear evidence for a significant scale-dependence of the bias (evaluated in redshift space) in the Stromlo-APM sample (Loveday et al. 1995) as

well as in the SSR S1 (Santiago & da Costa 1990) survey, but the real-space analysis of the former sample hints at some effect.

In general, the morphological segregation can not be caused by a possible luminosity segregation (with luminous galaxies clustering stronger than dim galaxies). As a matter of fact, the shape of the luminosity function of the E-S0 galaxies does not differ appreciably from that of Sp galaxies. Moreover, there are no large differences between the shapes of the type-specific luminosity functions, except for the earliest (E) and latest (Sm-Im) types (see Paper II).

6. Luminosity Segregation

Several investigations concerned with luminosity segregation looked particularly at a sequence of volume-limited samples and compared the amplitudes of the corresponding CFs. An increasing amplitude of CF with growing depth of the sample is in general considered as an indication of luminosity segregation (with luminous galaxies having a stronger clustering than dim objects). We have verified that this tendency is clearly apparent also in the NOG volume-limited samples. However, the results can be affected by the fact that one compares the clustering of low-luminosity and high-luminosity galaxies in very different volumes (the former objects are necessarily closer to us than the latter ones). The rise of the CF amplitude with the depth of the sample could be explained even in terms of a fractal model for the galaxy distribution, with no luminosity segregation, as shown by Pietronero (1987).

Therefore, we have decided to look for luminosity segregation by comparing the clustering of galaxies of different luminosities within the same volume-limited sample.

First we consider the volume-limited sample with depth of 6000 km/s. Figure 8 presents the CFs for the objects of different luminosity classes (-19.89 is the limiting value

of M_B of this volume-limited sample). Clearly, the CF amplitude decreases with decreasing luminosity, indicating a significant luminosity segregation. Table 3 shows the parameters resulting from the corresponding power-law fits together with the number density of galaxies n_g (for a completeness of 97%), and the mean intergalaxy distance d , calculated as $d = n_g^{-1/3}$.

Remarkably, the values of s_0 reported in Table 3 are significantly greater than the values predicted from the s_0 - d relationship, $s_0 = 0.4d$, proposed by Bahcall & West (1992) for a variety of galaxy systems. The departure from this relationship gets smaller for brighter galaxies, in agreement with Cappi et al.'s (1998) finding based on the SSSRS2 survey.

Figure 9 reveals that the relative biases between the above-mentioned subsamples of luminous galaxies and the least luminous ones is 1.5, 1.3 and 1.1, respectively. Clearly, these relative biases appear to be substantially constant with scale at least up to $10 h^{-1} \text{Mpc}$, in agreement with the contentions of Benoist et al. (1996) and Willmer et al. (1998). Consistently, a power spectrum analysis of volume-limited samples drawn from the CfA2 survey revealed a luminosity segregation with a luminosity bias independent of scale (Park et al. 1994).

As regards the volume-limited sample with depth of 5000 km/s, we subdivide the objects of this sample into three luminosity intervals, $M_B \leq -20.3$ ($N = 632$), $M_B = -19.89$ ($N = 1267$) and $M_B \geq -19.49$ ($N = 2220$) (the last value is the limiting M_B of the sample). Also in this sample we detect an appreciable luminosity segregation (see the plot of the corresponding CFs in Figure 10), with relative biases which are confirmed to be substantially constant with scale at least up to $10 h^{-1} \text{Mpc}$.

Analogously, we subdivide the objects of the volume-limited sample with depth of 4000 km/s into three luminosity intervals, $M_B \leq -19.89$ ($N = 624$), $M_B = -19.49$ ($N = 1107$),

$M_B = 19:01$ ($N = 1895$), and the objects of the volume-limited sample with depth of 3000 km/s into four luminosity intervals, the three mentioned below (comprising $N = 325$, 556, and 953 galaxies, respectively) and the interval $M_B = 18:39$. ($N = 1615$). The last M_B -intervals considered reach the limiting M_B -values of the samples.

We find no evidence of luminosity segregation below a luminosity corresponding to $M_B = 19:49$ mag, since the CFs relative to the low-luminosity intervals do not differ appreciably. We have checked that the removal of the galaxies belonging to the region of the Virgo cluster, which is the most prominent neighbor of G0 in the nearby ($cz < 3000$ km/s) universe, does not change this conclusion.

Repeating the same kind of analysis of the volume-limited samples for the E-S0 and the Sp objects, separately, we verify that the luminosity segregation holds separately for early- and late-type luminous ($M_B = 19:49$ mag) galaxies, whereas it is not present in the dim objects of both types. In conclusion, both early- and late-type galaxies show luminosity segregation, which, however, starts to appear only for luminous galaxies ($M_B < 19:5$ mag).

As in the case of morphological segregation (see x5), we wish to provide a further test of the luminosity segregation, considering specially two volume-limited samples at the depth of 6000 km/s, the samples of galaxies having $M_B = 19:89$ mag and $M_B = 20:6$ mag. According to the power-law fits reported in Table 3, the difference between the corresponding s_0 -values is significant at the 5% confidence level. We randomly select 499 galaxies from the former sample and compare its CF with that of the former sample. The two CFs are in general similar and, for 500 random selections, we can establish that the observed difference in the CF amplitudes of the two volume-limited samples (the mean ratio is 1.4 in the usual s -range) is significant at the 99.8% confidence level.

Our results are in line with a series of papers which, especially in the recent literature, reported evidence of diameter (Maurogordato et al. 1992) and luminosity segregation

(e.g., Hamilton 1988, Davis et al. 1988, Bommer, Mo, & Zhou 1989, Domínguez-Tenreiro & Martínez 1989, Park et al. 1994, Guzzo et al. 1997, Willmer et al. 1998; Benoist et al. 1996; see the last paper for a list of articles arguing against luminosity segregation).

But in the literature there is less consensus about the range of luminosities and the morphological types at which the effect occurs. For instance, to cite some earlier results which disagree with our findings, Loveday et al. (1995) claimed to detect luminosity segregation only for galaxies of relatively low luminosity within the Stromlo-APM sample. Specifically, the authors found no evidence for stronger clustering of objects with $L > L_{22-M_{bj}-20}$ compared to galaxies of intermediate luminosities ($20-M_{bj}-19$, $L < L_{22-M_{bj}-20}$) (except for a small effect observed for late-type galaxies only), whereas the latter objects were found to be more clustered than dim galaxies ($19-M_{bj}-15$, $L < L_{22-M_{bj}-20}$).

Hasegawa & Umemura (1993) claimed that, after correction of luminosities for internal extinction, the early- and late-type galaxies of the CfA1 survey show luminosity segregation of opposite sign (i.e. segregation and anti-segregation, respectively) so that this opposite behavior is responsible for a lack of luminosity segregation in the total sample. Beisbart & Kerscher (2000), who reanalyzed the SSRS2 data in the mathematical framework of marked point processes, found a scale-dependent luminosity segregation attributed mostly to early-type objects.

Interestingly, no luminosity segregation was found in the IRAS 1.2 Jy sample (Bouchet et al. 1993, Fisher et al. 1994) and in the PSCz sample (Szapudi et al. 2000). A possible explanation for the different behavior of optical and IRAS galaxy samples with respect to luminosity is that the optical magnitudes are likely to be more strongly related to the mass than far-infrared fluxes.

The dissimilarity between optical and IRAS samples of galaxies (and spirals) can be evidenced by the fact that only 53% of NOG galaxies are common to the PSCz; moreover,

30% of the PSCz objects contained in the volume encompassed by the NOG has no counterparts in the NOG.

Lets us inspect the sample of very luminous galaxies (hereafter VLG), i.e. the objects with $M_B \leq -21 \text{ mag}$ ($> 2.4 L$) (see Table 3). The morphological mix of our VLG sample differs from that of the whole NOG sample, because the former sample comprises a larger fraction of E-S0 galaxies (26% versus 15%) and a smaller proportion of Scd galaxies (39% versus 53%). Compared to the whole NOG sample, there are fewer VLG objects among field (ungrouped) galaxies. For instance, for the H groups, the fraction of VLG objects which are field galaxies, members of pairs, members of groups with at least 3, 10, and 20 members is 18%, 22%, 60%, 26%, and 15%, respectively (for the whole NOG, the corresponding values are 39%, 17%, 44%, 20%, and 13%). Moreover, we count 21 (10%) VLG objects among members of the poor and rich clusters identified within the NOG (i.e., A 194, A 262, A 569, A 3229, A 3565, A 3574, A 3656, A 3742, Centaurus, Dorado, Eridanus, Fornax, Hydra, Ursa Major, Pegasus, Virgo; see Table 5 of Paper III); these systems comprise 10% of NOG galaxies. The three richest clusters (richness class 1) in the NOG volume (Virgo, Hydra, A 3565) comprise 6 (3%) VLG objects and 5% of NOG galaxies. Finally, if we count the number of VLG objects and the total number of galaxies belonging to the few systems which have the largest velocity dispersions (e.g. $\sigma_v > 400 \text{ km/s}$) and virial masses (e.g., $M_v > 10^{14} h^{-1} M_\odot$), we find again similar percentages (see x8.1 and x8.3 for the calculation of the two above-mentioned quantities).

Hence, VLG reside preferentially in galaxy systems (pairs and groups), though not predominantly in rich systems like galaxy clusters. Consistently, they show a value of s_0 (see Table 3) which is likely to be consistent with that of fairly rich groups, but it is still lower, though not by much, than that of clusters. We have checked that, if we define the VLG as the objects with M_B brighter than values ranging from -21.1 to -21.5 mag ($> 3.8 L$), we

obtain CFs of similar amplitudes.

Our results on VLG are in partial agreement with those by Cappi et al. 1998, who, examining the VLG objects (with $M_{bj} < -21$ mag, $L > 4L_{bj}$) extracted from the SSRS2 redshift survey, stated that these objects are not preferentially located in bona fide clusters, but stressed the similarity between their correlation length (for which they obtained $s_0 = 16 \pm 2 h^{-1} \text{ Mpc}$) and that of APM clusters of low richness (for which $s_0 = 14 h^{-1} \text{ Mpc}$ according to Dalton et al. 1994 and Croft et al. 1997).

7. The correlation function of NOG groups

In general the redshift distributions of relatively rich P and H groups are shifted to smaller values than that of galaxies. However, we have verified that the redshift distributions of the 506 P groups with $n = 3$ members, the 474 H groups with $n = 3$, the 280 and 189 H groups with $n = 4$ and 5 members, respectively, are not significantly different from that of galaxies, according to the nonparametric Kolmogorov-Smirnov (KS) statistical test (e.g., Hoel 1971). Therefore, we have computed the CF for these groups, assuming the same selection function adopted for galaxies. The same assumption was made by Ramella et al. 1990, Trasarti-Battistoni et al. 1997, and Girardi et al. 2000.

In Figure 11 we show the weighted CFs for P groups (with $n = 3$), H groups (with $n = 3$ and 5) and all galaxies. On small scales ($< 3.5 h^{-1} \text{ Mpc}$) the CF of groups starts dropping because of the anti-correlation due to the typical size of groups, whereas on large scales ($> 20 h^{-1} \text{ Mpc}$) the signal-to-noise ratio of CF appreciably decreases. Thus, we limit our following analysis to the separation interval $3.5 \leq r \leq 20 h^{-1} \text{ Mpc}$. The CFs of groups have larger amplitudes than that of galaxies, especially for the H groups with $n = 4$ and $n = 5$ members. Over the above-mentioned interval of separations, the mean value $\langle r \rangle$ of the

ratios (11 values) between the CF of groups and that of galaxies turns out to be 1.52 ± 0.32 and 1.97 ± 0.80 for the P and H groups with $n = 3$, respectively, and somewhat larger, i.e. 2.40 ± 0.70 , 2.36 ± 0.54 , for the H groups with $n = 4$ and 5 , respectively. These numbers do not change much, if we calculate the ratios using a different number of points over a similar interval of separations. According to these results, the excess of clustering of groups with respect to that of galaxies is significant at the 2σ confidence level.

Our results appear to be in good agreement with those by Girardi et al. (2000), who found $\langle r \rangle = 1.6$ for their total and volume-limited samples of percolation groups with $n = 3$ members. Our results are also compatible with those by Trasarti-Battistoni et al. (1997), who found $\langle r \rangle = 2$ for their total sample of percolation groups with $n = 3$ members selected in the Perseus-Pisces region above a similar number density threshold (110). These authors noted that the degree of clustering of percolation groups is insensitive to the choice of the velocity link parameter, but is a little sensitive to the distance link parameter adopted (values denoting much greater density contrast yield a stronger clustering).

The unweighted CFs of all groups and galaxies are smaller than the corresponding weighted CFs and are equal within 1σ errors. Hence distant groups, which are, on average, more luminous and more massive, are more strongly correlated than nearby groups.

Exploiting the volume-limited samples of groups and galaxies (at the depth of 4000 km/s), we can extend this kind of analysis to the relatively rich groups. In Figure 12 we show the CFs for the P groups with $n = 3, 5$ members and for galaxies. Groups (especially those with $n = 5$ members) again tend to show a stronger clustering than galaxies, although, because of the large errors involved, the effect is not very significant. Table 4 presents the mean value of the ratio $\langle r \rangle$ calculated for the above-mentioned interval of separation.

In order to evaluate the significance of the difference in clustering between groups and galaxies irrespective of the number of bins in which we divide a given interval of separations,

we have rebinned the pair counts considering the wide interval $0.5 \leq \log s \leq 1.1 \text{ h}^{-1} \text{ Mpc}$. Table 5 lists the amplitudes of the $\xi(s)$ (together with the 1σ errors) calculated at the mean value of the above-mentioned interval, $\log s = 0.8$ (i.e. $s = 6.31 \text{ h}^{-1} \text{ Mpc}$) for the magnitude-limited (m1) samples and volume-limited (vl) samples of groups and galaxies mentioned above. This table confirms an excess of clustering of groups with respect to galaxies at the 1σ confidence level, especially for groups with $n \geq 4$ members.

Using a power-law fit over the interval $3.5 \leq s \leq 20 \text{ h}^{-1} \text{ Mpc}$ for the weighted CF of the total sample of groups, we obtain $s_0 = 8.4 \pm 0.7 \text{ h}^{-1} \text{ Mpc}$ ($7.8 \pm 0.4 \text{ h}^{-1} \text{ Mpc}$), $\alpha = 1.3 \pm 0.2$ (2.0 ± 0.2) for the total sample of H groups (P groups) with $n \geq 3$ members, $s_0 = 9.4 \pm 1.0 \text{ h}^{-1} \text{ Mpc}$, $\alpha = 1.6 \pm 0.3$ for the H groups with $n \geq 4$ members, $s_0 = 9.8 \pm 1.2 \text{ h}^{-1} \text{ Mpc}$, $\alpha = 1.7 \pm 0.4$ for the H groups with $n \geq 5$ members. The corresponding values of α_8 are 1.2 ± 0.1 (1.4 ± 0.2), 1.4 ± 0.2 , 1.6 ± 0.3 , respectively.

Given the formal errors and the variations among results coming from different group samples, we can conclude that the slope of the CF of groups is not inconsistent with that of galaxies (the above-mentioned results point to a mean value of $\alpha = 1.6$), whereas s_0 is clearly greater than that of galaxies (at nearly the 3σ confidence level) and ranges from $s_0 = 8 \text{ h}^{-1} \text{ Mpc}$ (for groups with $n \geq 3$) to $s_0 = 10 \text{ h}^{-1} \text{ Mpc}$ (for $n \geq 5$).

The strength of clustering of the P and H groups does not differ significantly.

Our results agree with those reported by Girardi et al. (2000) for their volume-limited sample of groups at the depth of 7800 km/s . For this sample, which has a median velocity dispersion of $\sigma_v = 214 \text{ km/s}$, the authors found $s_0 = 8 \pm 1 \text{ h}^{-1} \text{ Mpc}$ and $\alpha = 1.9 \pm 0.7$. These numbers are very close to those given above for the P groups with $n \geq 3$ members.

The fact that richer ($n \geq 5$ members) groups have a CF of greater amplitudes than poorer groups ($n \geq 3$ members) is likely to be mostly due to an appreciable component of

spurious groups among the latter, since spurious groups should cluster like field galaxies. As a matter of fact, N -body simulations showed that an appreciable fraction of the poorer groups, those with $n < 5$ members, is false (i.e. unbound density fluctuations), whereas the richer groups almost always correspond to real systems (e.g., Ramella et al. 1997; Frederic 1995 a, b), as indicated also by optical and X-ray studies (e.g., Ramella et al. 1995; Mahdavi et al. 1997). Part of the difference in the degree of clustering of richer and poorer groups might be due to the existence of relationship between the strength of clustering and the system's richness. This relationship has been discussed for a variety of systems by several authors (e.g., Bahcall & West 1992; Croft et al. 1997). The system's richness is usually taken as a rough tracer of the system's mass, which is the physical quantity related to the predictions of cosmological models.

As regards the volume-limited samples of groups, power-law fits for the CF over the $3.5 \leq s \leq 20 h^{-1} \text{ Mpc}$ range give, for instance, $s_0 = 5.5 \pm 0.8 h^{-1} \text{ Mpc}$, $\gamma = 1.6 \pm 0.4$ ($s_0 = 5.6 \pm 0.8 h^{-1} \text{ Mpc}$, $\gamma = 1.5 \pm 0.3$) for the H (P) groups with $n \geq 3$ members which are characterized by a number density $n_g = 8 \cdot 10^4 h^3 \text{ Mpc}^{-3}$ and a mean intergroup separation $d = n_g^{-1/3} = 11 h^{-1} \text{ Mpc}$. Moreover, we obtain $s_0 = 6.0 \pm 1.8 h^{-1} \text{ Mpc}$, $\gamma = 1.6 \pm 0.7$ ($s_0 = 7.3 \pm 1.4 h^{-1} \text{ Mpc}$, $\gamma = 1.6 \pm 0.5$), on scales $3.5 \leq s \leq 30 h^{-1} \text{ Mpc}$, for the H (P) groups with $n \geq 5$ members, which are characterized by a number density $n_g = 3 \cdot 10^5 h^3 \text{ Mpc}^{-3}$ and a mean intergroup separation $d = 15 h^{-1} \text{ Mpc}$. These results confirm that s_0 tends to increase with the number of group members, although there is only a marginal difference with respect the CF amplitude of the corresponding volume-limited sample of galaxies, for which a power-law fit (over the $2.7 \leq s \leq 12 h^{-1} \text{ Mpc}$ range) gives $s_0 = 5.09 \pm 0.10 h^{-1} \text{ Mpc}$, $\gamma = 1.64 \pm 0.08$.

The above-mentioned values of s_0 and d for the volume-limited samples of groups are not far from the $s_0 = 0.4d$ relationship proposed by Bahcall & West (1992). Specifically,

they agree with the $s_0 - d$ curves predicted by N-body cosmological simulations which reproduce the observed $s_0 - d$ relation of galaxy clusters (especially in the case of low-density (open) CDM ; cf. Figure 8 of Governato et al. 1999).

8. The Dependence of the Group Correlation Function on Group Properties

In this section we wish to check on a possible dependence of the strength of clustering of groups on some properties of groups, such as the velocity dispersion, the virial radius, the mean pairwise separation of group members, the virial mass, the crossing time, and the morphological composition of group members.

8.1. Velocity Dispersion

First, we have computed the line-of-sight velocity dispersion σ_v , which for a spherical system is smaller by $\sqrt{3}$ than the 3D velocity dispersion. Specifically, we have estimated the "robust" velocity dispersion by using the biweight estimator for rich groups ($n \geq 15$) and the gapper estimator for poorer groups (see the ROSTAT routines by Beers, Flynn, & Gebhardt 1990). Beers et al. (1990) have discussed the superiority of these techniques in terms of efficiency and stability when systems with a small number of members are analyzed (cf. also Girardi et al. 1993). We have applied the relativistic correction and the standard correction for velocity errors (Danese, De Zotti, & di Tullio 1980), adopting a typical velocity error of 30 km/s for each galaxy. This error is the average of the mean errors estimated in the RC3 catalog (de Vaucouleurs et al. 1991) for optical and radio radial velocities. For a few groups, corrections for velocity errors lead to $\sigma_v = 0$.

In general, the σ_v -distribution of P groups is shifted to greater values than that of H groups. The medians of σ_v are 129 and 83 km/s for the respective groups with $n \geq 3$

members and tend to increase as we go to richer groups (e.g. the respective medians are 161 and 106 km/s for the groups with $n \geq 5$ members). The P and H LEDA groups identified by Garcia (1993) exhibit a similar difference, which is due to differences in the algorithms of group selection (the v -medians are 151 and 118 km/s for the P and H LEDA groups with $\log n > 20$; see Girardi & Giuricin 2000). The v -median of the NOG H groups is in substantial agreement with the corresponding medians of other catalogs of groups selected with the H algorithm, the PGC groups (73 km/s; see Gourgoulhon, Chamaraux, & Fouque 1992) and NBG groups (100 km/s; see Tully 1987). As for the P algorithm, the v -median of the NOG P groups is close to the value of the revised CfA1 groups (116 km/s; Nolthenius 1993), in which a restrictive velocity link parameter was used, and quite smaller (as expected) than the medians of 170–200 km/s relative to samples of groups in which generous velocity link parameters were adopted (e.g. the CfA2 north groups by Ramella, Pisani, & Geller 1997, the PPS groups by Trasarti-Battistoni 1998, the ESP groups by Ramella et al. 1999, the SSR S2 groups by Ramella et al. 2000).

We divide the NOG P and H groups into two subsamples of equal sizes, i.e. groups with v greater and smaller than the median values. In general, the redshift distributions of the earlier group subsets are shifted to greater values than those of the latter subsets, except in the case of P groups with $n \leq 3$ members. Therefore, for this group sample, we can compare the weighted CFs of the group subsets relative to high and low v -values (see Figure 13). High- v groups are more clustered than their low- v counterparts. Adopting the above-mentioned rebinning procedure, we find $\langle s \rangle = 0.76^{+0.26}_{-0.28}$ and $1.61^{+0.41}_{-0.52}$ for the low- v and high- v groups, respectively. This leads to a > 1 significant difference. Using a power-law fit over the usual interval of separations we obtain $s_0 = 8.6 \pm 0.3 \text{ h}^{-1} \text{ Mpc}$, $\alpha = 2.1 \pm 0.3$ for the high- v groups and $s_0 = 5.3 \pm 1.5 \text{ h}^{-1} \text{ Mpc}$, $\alpha = 1.4 \pm 0.5$ for the low- v groups.

Then we have subdivided the volume-limited samples of groups on the basis of the medians of \bar{v} . Table 6 reports the values of the \bar{v} evaluated at s for the volume-limited H and P groups with $n = 3$ and $n = 4$. In this table we denote by \bar{v}_y the limiting value adopted for subdividing the each sample of groups into two subsamples, i.e. the groups with high and low \bar{v} . We confirm an excess of clustering (at the 1-2 confidence level) for systems of relatively high \bar{v} -values in the case of H groups. The volume-limited P groups (with $n = 3$ and $n = 4$) show a weak tendency in the same sense, which is, however, not statistically significant.

For these groups we have also calculated the distributions of pairwise group separations. We find that the two distributions relative to the high- \bar{v} and low- \bar{v} P groups with $n = 4$ members differ at the 99.9% confidence level according to the K-S test; in other words, high- \bar{v} groups have a distribution shifted to lower values than the other groups, as is expected from their greater degree of clustering. For the H groups the corresponding difference is significant at the 98.3% confidence level. No appreciable difference (i.e. no difference at the $> 90\%$ confidence level) is seen for the P and H groups with $n = 3$ members.

8.2. Virial Radius and Mean Pairwise Separation

We have computed the projected virial radius R_{pv} as $R_{pv} = n(n-1)^{-1} \sum_{i>j}^P R_{ij}^2$ where R_{ij} is the projected distance between galaxies and n the number of group members. For a spherical system the projected virial radius is smaller by $\sqrt{2}$ than the virial radius R_v . We have computed the mean pairwise member separation R_m as $(4\pi)^{-1} \langle R_{ij}^2 \rangle$ where 4π is the projection factor. R_m is likely to be a more robust estimate of the group size than the virial radius.

The H groups have typically greater values of R_m and R_{pv} than the P groups. The R_{pv} (R_m)-medians are 0.60 (0.65) and 0.48 (0.50) $h^{-1} Mpc$ for the respective groups with $n = 3$ members and tend to increase as we go to richer groups (e.g., the respective medians are 0.66 (0.78) and 0.52 (0.57) $h^{-1} Mpc$ for the groups with $n = 5$ members). The NOG P groups have smaller sizes than the LEDA P groups (the LEDA H and P groups have a R_{pv} -median of 0.62 $h^{-1} Mpc$; see Girardi & Giuricin 2000) and the new UZC groups by Pisani et al. 2001 (which have a R_{pv} -median of 0.64 $h^{-1} Mpc$), probably because we have adopted smaller link parameters. Other catalogs of H and P groups are not easily comparable to the NOG groups in this respect, because in general the authors (e.g. Ramella et al. 1997) calculate the harmonic radius, which is systematically smaller than the virial radius by a factor of ~ 2 (as discussed by Giuricin 1989).

Since the redshift distributions of the high- R_{pv} and high- R_m groups is considerably shifted to greater values than that of the low- R_{pv} and low- R_m groups, we consider only the volume-limited samples of groups in the analysis of the dependence of CF on R_{pv} and R_m .

Subdividing the volume-limited samples of groups according to the medians of R_{pv} and R_m , we find that the high- R_{pv} and high- R_m groups (with $n = 3, n = 4, n = 5$) tend to be more clustered than the low- R_{pv} and low- R_m counterparts. As in the case of ξ , the effect is more pronounced for H groups than for P groups. Moreover, the effect gets stronger if we increase the limiting value of R_{pv} (R_m) so as to subdivide the groups into a high- R_{pv} (R_m) sample containing $\sim 1/3$ of groups and a low- R_{pv} (low- R_m) sample comprising $\sim 2/3$ of groups. Figure 14 shows the ξ (s) of the high- R_{pv} and low- R_{pv} H groups (with $n = 4$). Table 7 contains the values of ξ (s) calculated after rebinning. In this table R_{pv}^Y and R_m^Y are the limiting values adopted for subdividing each sample of groups into two subsamples of high and low size. Table 7 reveals that the statistical significance of this effect is at the $1 - 2$ level. For the volume-limited samples of P and H groups, this effect is respectively slightly

larger and smaller than the effect related to σ_v .

8.3. Virial Mass

We have calculated the virial mass M_v as $M_v = 3 \cdot (\sigma_v)^2 R_{pv} / G$. (M_v has not been calculated in systems having $\sigma_v = 0$). For a system which is virialized and which has a mass distribution similar to the galaxy distribution, the virial mass is a reliable indicator of the mass.

Reflecting the difference in σ_v , the P groups are, on average, more massive than the H groups. The M_v -medians are $8.7 \cdot 10^2 h^{-1} M_\odot$ and $5 \cdot 10^2 h^{-1} M_\odot$ for the respective groups with $n = 3$ and increase as we go to richer systems (e.g. the respective medians are $1.4 h^{-1} 10^{13} M_\odot$ and $7.8 h^{-1} M_\odot$ for the groups with $n = 5$ members). The P and H LEDA groups exhibit an even larger difference in the same sense between the M_v -medians ($14.8 \cdot 10^2 h^{-1} M_\odot$ and $6.6 \cdot 10^2 h^{-1} M_\odot$, respectively; see Girardi & Giuricin 2000), because of differences in the typical sizes of P and H groups discussed in the previous subsection.

As in the case of R_{pv} and R_m , since the redshift distribution is related to M_v , we consider only the volume-limited samples of groups in examining the dependence of CF on M_v .

Subdividing the groups according to the M_v -medians, we find that the more massive groups tend to be more clustered than the less massive ones, that this effect is more pronounced for the H groups than for the P groups and gets stronger if we raise the limiting values of M_v above their medians. These results are parallel to those found for σ_v and (especially) for R_{pv} , as expected from the dependence of M_v on these two quantities. Figures 15 and 16 illustrates the CFs of the high- M_v and low- M_v groups. Table 8, which

reports the values of $\langle s \rangle$ for P and H groups with high and low M_v -values (compared to the value denoted by M_v^y) and $n = 3$ and 4 members, reveals that this effect is in general not stronger than the effect on σ_v and on R_{pv} for the volume-limited H and P groups, respectively.

The comparison of the distributions of pairwise group separations of the above-mentioned samples of groups reveals that high- M_v groups have always lower separations, on average, than the corresponding low- M_v groups, with a statistical significance ranging from 95.1% to 99.99% confidence level.

Most of galaxy groups are indeed in the phase of collapse and not yet virialized (e.g. Giuricin et al. 1988, Pisani et al. 1992). Corrections for non-virialization effects lead to masses which are greater than virial masses by 20-60%, depending on the group catalog and on the assumed cosmology (Girardi & Giuricin 2000). However, the corrected masses correlate very well with the (uncorrected) virial masses. Therefore, these corrections have no effect on the analysis described in this subsection.

8.4. Virial Crossing Time

We have calculated the virial crossing time t_{cr} (expressed in units of the Hubble time t_H) as $t_{cr} = (3/5)^{3/2} [R_{pv}/\sigma_v]^{1/2}$ (see Giuricin et al. 1988 for further details). Owing to the difference in the values of σ_v and R_{pv} , the H groups have, in general, larger t_{cr} -values than the P groups. The t_{cr} -medians are 0.29 and 0.18 for all H and P groups, respectively, with the redshift distribution of the high- t_{cr} P groups being shifted to greater values with respect to that of low- t_{cr} groups. We have detected no appreciable difference between the $\langle s \rangle$ of high- and low- t_{cr} H and P groups, for the total and volume-limited samples. Clearly, since $t_{cr} / R_{pv} = \sigma_v$, the above-mentioned effects on R_{pv} and σ_v cancel out in the ratio.

8.5. Morphological Composition

We have calculated the fraction of early-type (E+S0) galaxies for the NOG groups. The median fraction is 0.2 for the total and volume-limited samples of H and P groups. As expected from the morphological segregation, this fraction is greater than the fraction of 15% which refers to the whole NOG.

Groups having a small fraction of early-type galaxies are in general nearer than the norm. We have detected no appreciable difference between the CF's of the H and P groups with small and large fractions of early-type galaxies for the total and volume-limited samples.

9. Summary and Conclusions

Using the two-point correlation function in redshift space, we study the clustering of the galaxies and groups of the Nearby Optical Galaxy (NOG) sample, which is a complete, distance-limited ($cz \leq 6000$ km/s) and magnitude-limited sample of 7000 nearby and bright optical galaxies, which covers 2/3 of the sky ($b_j > 20^\circ$). We consider two catalogs of NOG groups identified through the hierarchical and percolation algorithms.

Our main results can be summarized as follows:

- 1) The redshift-space two-point correlation function of NOG galaxies can be well described by a power-law, with slope $\gamma = 1.5$ and correlation length $s_0 = 6.4 h^{-1}$ Mpc between 2.7 and $12 h^{-1}$ Mpc, in substantial agreement with the results of most redshift surveys of optical galaxies. Optical surveys, characterized by quite different geometries, volumes, and selection criteria, exhibit similar galaxy correlation functions (at least between 2 and $20 h^{-1}$ Mpc), although they show significant discrepancies in the shape and normalization of the resulting galaxy luminosity functions (as discussed in Paper II). The

agreement between galaxy correlation functions derived for a wide range of volumes and sample radii (as defined in Guzzo 1997) is in contrast with the fractal interpretation of the galaxy distribution in the universe.

2) Subdividing the NOG into early-type (E-S0) and late-type (spirals and irregular) galaxies, we note a pronounced morphological segregation, out to $20h^{-1} \text{ Mpc}$, between the former objects (characterized by $s_0 = 11 h^{-1} \text{ Mpc}$ and $\gamma = 1.5$) and the latter ones (characterized by $s_0 = 5.6 h^{-1} \text{ Mpc}$ and $\gamma = 1.5$), in qualitative agreement with many previous investigations. Remarkably, the morphological segregation persists also at relatively low luminosities ($M_B > -19 \text{ mag}$).

Subdividing further the NOG into several morphological subtypes, we note a gradual increase of the strength of clustering from the late-type spirals to the S0s, especially on intermediate scales (around $5h^{-1} \text{ Mpc}$).

The relative bias factor (≈ 1.7 in redshift space) between early- and late-type objects, for which there is no good agreement in the literature, appears to be substantially constant with scale. However, this result is not incompatible with a possible scale dependence in the relation between galaxy number density and mass density (see, e.g., Blanton et al. 1999).

3) Analyzing different volume-limited samples, we find that the luminous galaxies turn out to be more clustered than the dim objects. The luminosity segregation, which is significant for both early- and late-type objects, starts to become appreciable only at relatively high luminosities ($M_B < -19.5$, i.e. $L > 0.6 L^*$) and is independent on scale (at least up to $10h^{-1} \text{ Mpc}$).

The very luminous galaxies ($M_B < -20$; $L > 2.4 L^*$) reside preferentially in binaries and groups (though not in clusters) and their degree of clustering ($s_0 = 12 h^{-1} \text{ Mpc}$) is compatible with that of rich groups.

Both morphological and luminosity segregations are two separate effects (one effect is not generated by the other). The fact that they are present also on large scales favors the interpretation that, on scales greater than $\sim 1 h^{-1} \text{ Mpc}$, the bulk of these effects is likely to be mostly primordial in origin, i.e. inherent in schemes of biased galaxy formation (e.g. Bardeen et al. 1986) and not induced by late environmental effects (e.g. due to merging, harassment, tidal stripping, accretion, ram pressure).

4) The NOG groups identified with the H and P algorithms, though having somewhat different distributions of velocity dispersions, virial masses, and sizes, have similar clustering properties. The groups show a degree of clustering which is intermediate between those of galaxies and clusters. Compared to galaxies, they exhibit an excess of clustering by a factor 1.5 and 2, for groups with $n = 3$ and 5 members, respectively. The groups with $n = 3$ members are characterized by $s_0 \sim 8 h^{-1} \text{ Mpc}$, which should be regarded as a lower limit since poor groups can be appreciably contaminated by spurious groups. The groups with $n = 5$ members, which have typical (median) velocity dispersions of $\sigma_v \sim 100 - 150 \text{ km/s}$, virial radii of $R_v \sim 1 h^{-1} \text{ Mpc}$, and virial masses of $M_v \sim 10^{13} h^{-1} M_\odot$, are characterized by $s_0 \sim 10 h^{-1} \text{ Mpc}$.

5) The strength of group clustering depends on the physical properties of groups. Specifically, groups with greater velocity dispersions, sizes (as traced by virial radii and mean pairwise member separations), and virial masses tend to be more clustered than those with lower values of these quantities. The H groups display a slightly stronger effect than the P groups. On the other hand, there is no difference in the degree of clustering between groups with small and large proportion of early-type galaxies.

In comparing the results from different samples through the analysis of correlation functions in redshift space, we have adopted the working hypothesis that, to first order, the influence of redshift space distortions will affect the samples being compared in similar

ways. We are undertaking the analysis of the real-space clustering in the NOG. The results of this work, which is in progress, will be presented in a forthcoming paper.

Our results can provide useful constraints to current models of galaxy formation, which are able to fit the two-point galaxy correlation function in a Λ CDM cosmology (e.g., Benson et al. 2000) and also attempt to reproduce, with a limited success, the observed morphological and luminosity segregation (e.g., Kauffmann et al. 1999). As for the clustering of groups, our findings can offer some additional constraints for N-body simulations which in different cosmologies predict the clustering properties of galaxy systems (see, e.g., Governato et al. 1999 and Colberg et al. 2000 for recent relevant accounts).

We are grateful to L. Guzzo, who have sent us some data, and we thank S. Borgani, F. Marrirossian, P. Monaco, M. Ramella for interesting conversations.

S.S. acknowledges receipt of a grant of the University of Trieste and a TRIL fellowship of the International Center for Theoretical Physics of Trieste.

This work has been partially supported by the Italian Ministry of University, Scientific and Technological Research (MURST) and by the Italian Space Agency (ASI).

R E F E R E N C E S

- Andreon, S., Davoust, E., & Heim, T. 1997, *A & A*, 323, 337
- Bahcall, N. A. & Soneira, R. M. 1983, *ApJ* 270, 20
- Bahcall, N. A. & West, M. J. 1992, *ApJ*, 392, 419
- Bardeen, J. M., Bond, J. R., Kaiser, N., Szalay, A. S. 1986, *ApJ*, 304, 15
- Beers, T. C., Flynn, K., & Gebhardt, K. 1990, *AJ*, 100, 32
- Beisbart, C. & Kerscher, M. 2000, *ApJ*, 545, 6.
- Benoist, C., Maurogordato, S., da Costa, L. N., Cappi, A., Schaefer, R. 1996, *ApJ*, 472, 452
- Benson, A. J., Cole, S., Frenk, C. S., Baugh, C. M., Lacey, C. G. 2000, *MNRAS*, 311, 793
- Bhavsar, S. P. 1981, *ApJ*, 246, L5
- Blanton, M., Cen, R., Ostriker, J. P. & Strauss, M. A. 1999, *ApJ*, 522, 590
- Borgani, S., Plionis, M., & Kolokotronis, V. 1999, *MNRAS*, 305, 866
- Bomer, G., Mo, H. J., & Zhou, Y. 1989, *A & A*, 221, 191
- Bouchet, F. R. et al. 1993, *ApJ*, 417, 36
- Cappi, A., da Costa, L. N., Benoist, C., Maurogordato, S. & Pellegrini, P. S. 1998, *AJ*, 115, 2250
- Colberg, J. M. et al. 2000, *MNRAS*, 319, 209
- Croft, R. A. C., Dalton, G. B., Efsthathiou, G., Sutherland, W. J., Maddox, S. J. 1997, *MNRAS*, 291, 305
- Dalton, G. B. et al. 1994, *MNRAS*, 271, L47
- Danese, L., De Zotti, G., & di Tullio, G. 1980, *A & A*, 82, 322
- Davis, M. & Djorgovski, S. 1985, *ApJ*, 299, 15

- Davis, M. & Geller, M. J. 1976, *ApJ*, 208, 13
- Davis, M. & Huchra 1982, *ApJ*, 254, 437
- Davis, M., Meiksin, A., Strauss, M. A., da Costa, L. N. & Yahil, A. 1988, *ApJ*, 333, L9
- Davis, M. & Peebles, P. J. E., 1983, *ApJ*, 267, 465
- de Lapparent, V., Geller, M. J., & Huchra, J. P. 1988, *ApJ*, 332, 44
- de Lapparent, V., Geller, M. J., & Huchra, J. P. 1989, *ApJ*, 343, 1
- de Souza, R. E., Capelato, H. V., Arakaki, L. & Loguillo, C. 1983, *ApJ*, 263, 557
- de Vaucouleurs, G. et al. 1991, *Third Reference Catalogue of Bright Galaxies* (New York: Springer)
- Domínguez-Tenreiro, R. & Martínez, V. J. 1989, *ApJ*, 339, L9
- Domínguez-Tenreiro, R., Campos, A., Gómez-Flechoso, M. A. & Yepes, G. 1994, *ApJ*, 424, L73
- Dressler, A. 1980, *ApJ*, 236, 351
- Dressler, A. et al. 1997, *ApJ*, 490, 577
- Ferguson, H. C. & Binggeli, B. 1994, *A & A Rev.*, 6, 67
- Fisher, K. B., Davis, M., Strauss, M. A., Yahil, A., Huchra, J. P. 1994, *MNRAS*, 266, 50
- Frederic, J. J. 1995a, *ApJS*, 97, 259
- Frederic, J. J. 1995b, *ApJS*, 97, 275
- Garcia, A. M. 1993, *A & AS*, 100, 47
- Giovanelli, R., Haynes, M., & Chincarini, G. 1986, *ApJ*, 300, 77
- Girardi, M., Biviano, A., Giuricin, G., Mardirossian, F. & Mezzetti, M. 1993, *ApJ*, 404, 38
- Girardi, M., Boschini, W., & da Costa, L. N. 2000, *A & A*, 353, 57

- G irardi, M . & G iuricin, G . 2000, ApJ, 540, 45.
- G iuricin, G . 1989, in M orphological C osm ology, ed. P . Flin & H . W . D uerbeck, Lecture Notes in Physics No. 332 (Berlin: Springer), 107
- G iuricin, G ., G ondolo, P ., M ardirossian, F ., M ezzetti, M . & R am ella, M . 1988, A & A , 199, 85
- G iuricin, G ., M arinoni, C ., Ceriani, L. & P isani, A . 2000, ApJ, 543, 178 (Paper III)
- G ourgoulhon, E ., Cham araux, P ., & Fouque, P . 1992, A & A , 255, 69
- G overnato, F . et al. 1999, M N R A S , 307, 949
- G uzzo, L . 1997, N ew A , 2, 517
- G uzzo, L ., Strauss, M . A ., Fisher, K . B ., G iovanelli, R . & Haynes, M . 1997, ApJ, 489, 37
- G uzzo, L . et al. 2000, A & A , 355, 1
- H am ilton, A . J. S. 1988, ApJ, 331, L59
- H am ilton, A . J. S. 1993, ApJ, 417, 19
- H asegawa, T . & U m em ura, M . 1993, M N R A S , 263, 191
- H erm it, S. et al. 1996, M N R A S , 283, 709
- H oel, P . G . 1971, Introduction to M athem atical Statistics (New York, W iley)
- Iovino, A ., G iovanelli, R ., Haynes, M ., Chincarini, G ., G uzzo, L . 1993, M N R A S , 265, 21
- Jing, Y . & Zhang, J., 1988, A & A , 190, L21
- K alinkov, M . & K uneva, I. 1990, IAU C olloq. 124, 149
- K au m ann, G ., Colberg, J. M ., D iaferio, A ., W hite, S. M . 1999, M N R A S , 303, 188
- K erscher, M ., Szapudi, I., & Szalay, A . S. 2000, ApJ, 535, L13
- Lahav, O . & Saslaw, W . C . 1992, ApJ, 396, 30

- Ling, E. N., Frenk, C. S. & Barrow, J. D. 1986, *MNRAS*, 223, 21P
- Loveday, J., Maddox, S. J., Efsthathiou, G. & Peterson, B. A. 1995, *ApJ*, 442, 457
- Mahdavi, A., Bohringer, H., Geller, M. J., Ramella, M. 1997, *ApJ*, 483, 68
- Mai, M. A. G. & da Costa, L. N. 1990, *ApJ*, 349, 477
- Marinoni, C., Monaco, P., Giuricin, G., Costantini, B. 1998, *ApJ*, 505, 484 (Paper I)
- Marinoni, C., Monaco, P., Giuricin, G., Costantini, B. 1999, *ApJ*, 521, 50 (Paper II)
- Marinoni, C., Hudson, M. J., & Giuricin, G. 2001, submitted.
- Maurogordato, S. & Lachieze-Rey, M. 1987, *ApJ*, 320, 13
- Maurogordato, S., Schaefer, R., & da Costa, L. N. 1992, *ApJ*, 390, 17
- Mo, H. J., Jing, Y. P., & Bomer, G. 1992, *ApJ*, 392, 452
- Nolthenius, R. 1993, *ApJS*, 85, 1
- Nolthenius, R. & White, S. D. M. 1987, *MNRAS*, 235, 505
- Park, C., Vogele, M. S., Geller, M. J., Huchra, J. P. 1994, *ApJ*, 431, 569
- Paturel, G. et al. 1997, *A&AS*, 124, 109
- Peacock, J. A. & West, M. J. 1992, *MNRAS*, 259, 494
- Peebles, P. J. E. 1980, *The Large-Scale Structure of the Universe* (Princeton: Princeton Univ. Press)
- Pietronero, L. 1987, *Phys. Rev. A*, 144, 257
- Pisani, A., Giuricin, G., Mardrossian, F., Muzzetti, M. 1992, *ApJ*, 389, 68
- Pisani, A. et al. 2001, in preparation
- Pons-Borderia, M.-J., Martinez, V. J., Stoyan, D., Stoyan, H. & Saar, E. 1999, *ApJ*, 523,

- Postman, M. & Geller, M. J. 1984, *ApJ*, 281, 95
- Postman, M., Huchra, J. P. & Geller, M. J. 1991, *ApJ*, 384, 404
- Ramella, M. et al. 1999, *A & A*, 342, 1
- Ramella, M. et al. 2000, in preparation
- Ramella, M., Geller, M. J., & Huchra, J. P. 1990, *ApJ*, 353, 51
- Ramella, M., Geller, M. J., & Huchra, J. P. 1992, *ApJ*, 384, 396
- Ramella, M., Geller, M. J., Huchra, J. P., Thorstensen, J. R. 1995, *AJ*, 109, 1469
- Ramella, M., Pisani, A., & Geller, M. J. 1987, *AJ*, 113, 483
- Ratcliffe, A. et al. 1996, *MNRAS*, 281, L47
- Santiago, B. X. & da Costa, L. N. 1990, *ApJ*, 362, 386
- Schechter, P. L. 1976, *ApJ*, 203, 297
- Seaborn, M. D. et al. 1999, *MNRAS*, 309, 89.
- Szapudi, I., Branchini, E., Frenk, C. S., Maddox, S., Saunders, W., 2000, *MNRAS*, 318, L45.
- Totsuji, H. & Kihara, Y. 1969, *PASJ*, 21, 221
- Trasarti-Battistoni, R. 1998, *A & AS*, 130, 341
- Trasarti-Battistoni, R., Invernizzi, G. & Bonometto, S. A. 1997, *ApJ*, 475, 1
- Tucker, D. L. et al. 1995, in *Clustering in the Universe*, ed. C. Balkowski et al. (Gif-sur-Yvette: Ed. Frontieres), 39
- Tucker, D. L. et al. 1997, *MNRAS*, 285, L5
- Tully, R. B. 1987, *ApJ*, 321, 280
- White, S. D. M., Tully, R. B., & Davis, M. 1988, *ApJ*, 333, L45

W illmer, C .N .A ., da Costa, L .N ., & Pellegrini, P .S . 1998, A J, 115, 869

Fig. 1. | The redshift-space galaxy correlation function from the whole NOG, compared to results from the Las Campanas (LCRS), Stromlo-APM, Durham-UKST, and ESP redshift surveys; 1 error bars are shown for the NOG correlation function.

Fig. 2. | Comparison between the weighted (open circles) and unweighted (dots) correlation functions for the whole NOG, and the correlation function for the volume-limited sample with depth of 6000 km/s (stars). For the sake of clarity, error bars are shown for the last case only.

Fig. 3. | The same as in Figure 3, but for samples limited at the depth of 4000 km/s.

Fig. 4. | Comparison of the correlation functions for the early-type (open diamonds) and late-type (open circles) galaxies of the whole NOG, and for the early-type (filled diamonds) and late-type (dots) galaxies of the magnitude-limited sample truncated at 4000 km/s. For the sake of clarity, errors bars are shown for one sample only.

Fig. 5. | Comparison of the correlation functions for the E (open circles), S0 (open diamonds), S0/a (open squares), and Sa (dots) morphological types of the whole NOG. For the sake of clarity, error bars are shown for the last sample only.

Fig. 6. | Comparison of the correlation functions for the Sa (dots), Sb (stars), and Scd (open circles) morphological types of the whole NOG. For the sake of clarity, error bars are shown for the first sample only.

Fig. 7. | The relative bias between early- and late-type galaxies in the NOG. A typical error bar is shown.

Fig. 8. | Comparison of the correlation functions for different subsamples of the volume-limited sample with depth of 6000 km/s. Each subsample corresponds to a given luminosity class. Error bars are shown for one subsample only.

Fig. 9. | The relative bias between the subsamples of galaxies of different luminosity classes considered in Figure 8. The bias is normalized to the value relative to the faintest subsample ($M_B = 19.89$ mag). A typical error bar is shown.

Fig. 10. | Comparison of the correlation functions for different subsamples of the volume-limited sample with depth of 5000 km/s. Each subsample corresponds to a given luminosity class. Error bars are shown for one subsample only.

Fig. 11. | Comparison of the correlation functions for the NOG galaxies (stars), the P groups with $n = 3$ members (diamonds), the H groups with $n = 3$ members (open circles), and the P groups with $n = 5$ members (open squares). Error bars are shown for one case only.

Fig. 12. | Comparison between the correlation functions for the the volume-limited samples (with depth of 4000 km/s) of galaxies (stars) and P groups with $n = 3$ (open circles) and $n = 5$ members (open squares).

Fig. 13. | Comparison between the correlation functions for all P groups with $n = 3$ members having velocity dispersion greater (open circles) and smaller (dots) than $\sigma_v = 129$ km/s.

Fig. 14. | Comparison between the correlation functions for the volume-limited sample (with depth of 4000 km/s) of the H groups with $n = 4$ members having projected virial radii greater (open circles) and smaller (dots) than $R_{pv} = 0.9 h^{-1} \text{ Mpc}$.

Fig. 15. | Comparison between the correlation functions for the volume-limited sample (with depth of 4000 km/s) of the P groups with $n = 4$ members having virial masses greater (open circles) and smaller (dots) than $M_v = 2.7 \cdot 10^3 h^{-1} M_\odot$.

Fig. 16. | Comparison between the correlation functions for the volume-limited sample

{ 48 {

(with depth of 4000 km/s) of the H groups with $n = 4$ members having virial masses greater (open circles) and smaller (dots) than $M_v = 1.5 \cdot 10^3 h^{-1} M_\odot$.

.

Table 1. Correlation function parameters for different morphologies from the whole NOG

type	N	range ($h^{-1} \text{M pc}$)	S_0 ($h^{-1} \text{M pc}$)	α	β	γ	δ	ϵ
E-S0	1036	2.7 – 12	11:1	0.5	1.5	0.1	1.6	0.1
Sp	5899	2.7 – 12	5:6	0.1	1.49	0.07	0.94	0.02
E	621	2.7 – 12	9:7	1.0	1.8	0.3	1.6	0.3
S0	415	2.7 – 12	10:9	1.3	1.6	0.3	1.7	0.3
S0/a	496	2.7 – 17	8:5	0.9	1.2	0.2	1.2	0.1
Sa	845	2.7 – 12	7:4	0.5	1.5	0.2	1.2	0.1
Sb	822	2.7 – 12	5:5	0.3	1.8	0.3	1.0	0.1
Scd	3736	2.7 – 12	5:1	0.2	1.5	0.1	0.88	0.03

Table 2. Correlation function parameters for different morphologies from the
volume-limited sample at 6000 km/s

type	N	range (h ⁻¹ Mpc)	S ₀ (h ⁻¹ Mpc)		s ₈			
E-S0	407	2.7–12	11.6	0.8	1.5	0.2	1.6	0.2
Sp	1826	2.7–12	6.4	0.2	1.5	0.1	1.04	0.03
E	297	2.7–12	10.5	1.0	1.6	0.2	1.6	0.2
S0	110	2.7–12	11.0	1.6	2.1	0.4	2.2	0.8
Sa	308	2.7–12	9.0	1.0	1.3	0.3	1.3	0.1
Sb	358	2.7–12	6.0	0.4	1.9	0.3	1.1	0.1
Scd	1059	2.7–12	5.5	0.2	1.4	0.1	0.92	0.02

Table 3. Correlation function parameters for different luminosity intervals

sample		N	range	s_0				δ		n_g		d
			(h ⁻¹ M pc)	(h ⁻¹ M pc)						(h ³ M pc ⁻³)		(h ⁻¹ M pc)
M _B	21:0	199	2.7 – 12	11:9	1:9	1:3	0:3	1:5	0:3	3:4	10 ⁴	14
M _B	20:6	584	2.7 – 12	8:7	0:3	1:6	0:1	1:4	0:1	1:0	10 ³	10
M _B	20:3	1119	2.7 – 12	7:8	0:2	1:5	0:1	1:21	0:04	1:9	10 ³	8
M _B	19:89	2257	2.7 – 12	7:2	0:2	1:5	0:1	1:14	0:03	3:9	10 ³	6

Table 4. The values of $\langle r \rangle$ for different samples of groups

sample	N	$\langle r \rangle$	
H groups (n = 3)	140	1:19	0:34
P groups (n = 3)	141	1:26	0:52
H groups (n = 4)	78	2:10	1:03
P groups (n = 4)	83	1:65	0:94
H groups (n = 5)	50	2:23	1:30
P groups (n = 5)	53	2:27	0:78
H groups (n = 6)	36	3:14	1:34
P groups (n = 6)	31	2:23	1:83
H groups (n = 7)	25	3:62	2:62
P groups (n = 7)	22	3:62	2:04

Table 5. Correlation function amplitudes for galaxies and groups

sample	ag	N	(s)
galaxies	m l	7028	$0.67^{+0.05}_{-0.06}$
P groups (n 3)	m l	506	$1.09^{+0.21}_{-0.25}$
H groups (n 3)	m l	474	$1.17^{+0.28}_{-0.27}$
H groups (n 4)	m l	280	$1.44^{+0.45}_{-0.43}$
H groups (n 5)	m l	189	$1.45^{+0.54}_{-0.57}$
galaxies	v l	1895	$0.46^{+0.03}_{-0.03}$
P groups (n 3)	v l	141	$0.69^{+0.17}_{-0.18}$
P groups (n 4)	v l	83	$0.90^{+0.29}_{-0.28}$
P groups (n 5)	v l	53	$1.07^{+0.43}_{-0.44}$
P groups (n 6)	v l	31	$0.69^{+0.54}_{-0.61}$
H groups (n 3)	v l	140	$0.61^{+0.16}_{-0.16}$
H groups (n 4)	v l	78	$0.98^{+0.34}_{-0.34}$
H groups (n 5)	v l	50	$0.96^{+0.45}_{-0.42}$
H groups (n 6)	v l	36	$1.53^{+0.51}_{-0.61}$

Table 6. Correlation function amplitudes for high- and low- v groups

sample	$\frac{y}{v}$ (km/s)	N	(s)
P groups (n 3, low v)	136.2	71	$0.46^{+0.20}_{-0.23}$
P groups (n 3, high v)	"	70	$0.79^{+0.31}_{-0.30}$
P groups (n 4, low v)	150.2	42	$0.78^{+0.51}_{-0.53}$
P groups (n 4, high v)	"	41	$1.17^{+0.47}_{-0.40}$
H groups (n 3, low v)	100.5	70	$0.35^{+0.26}_{-0.24}$
H groups (n 3, high v)	"	70	$0.99^{+0.35}_{-0.42}$
H groups (n 4, low v)	113.2	42	$0.34^{+0.31}_{-0.34}$
H groups (n 4, high v)	"	36	$2.55^{+0.84}_{-0.72}$

Note. | We denote by $\frac{y}{v}$ the limiting value adopted for subdividing each sample of groups into two subsamples of low and high v .

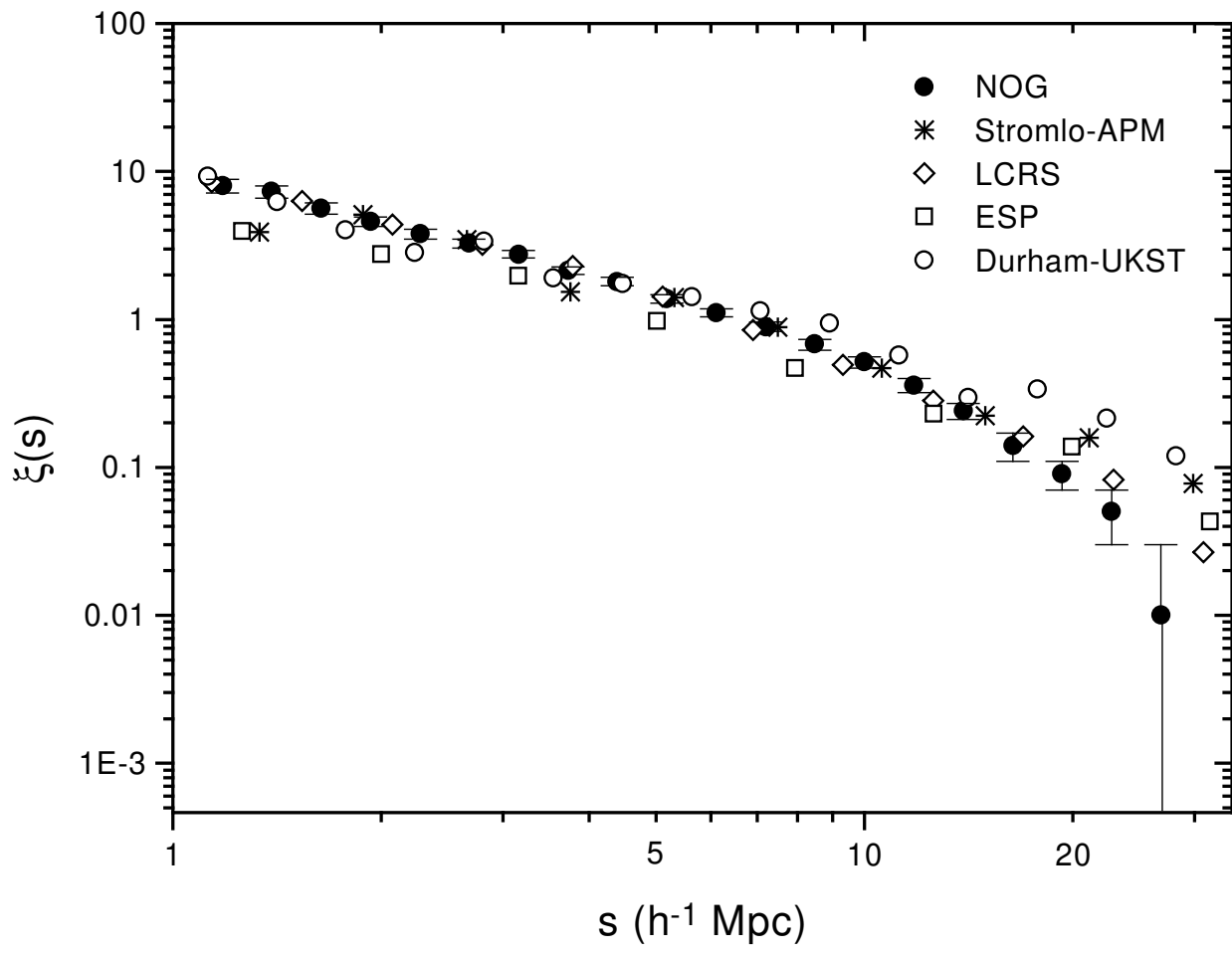
Table 7. Correlation function amplitudes for high- and low-size groups

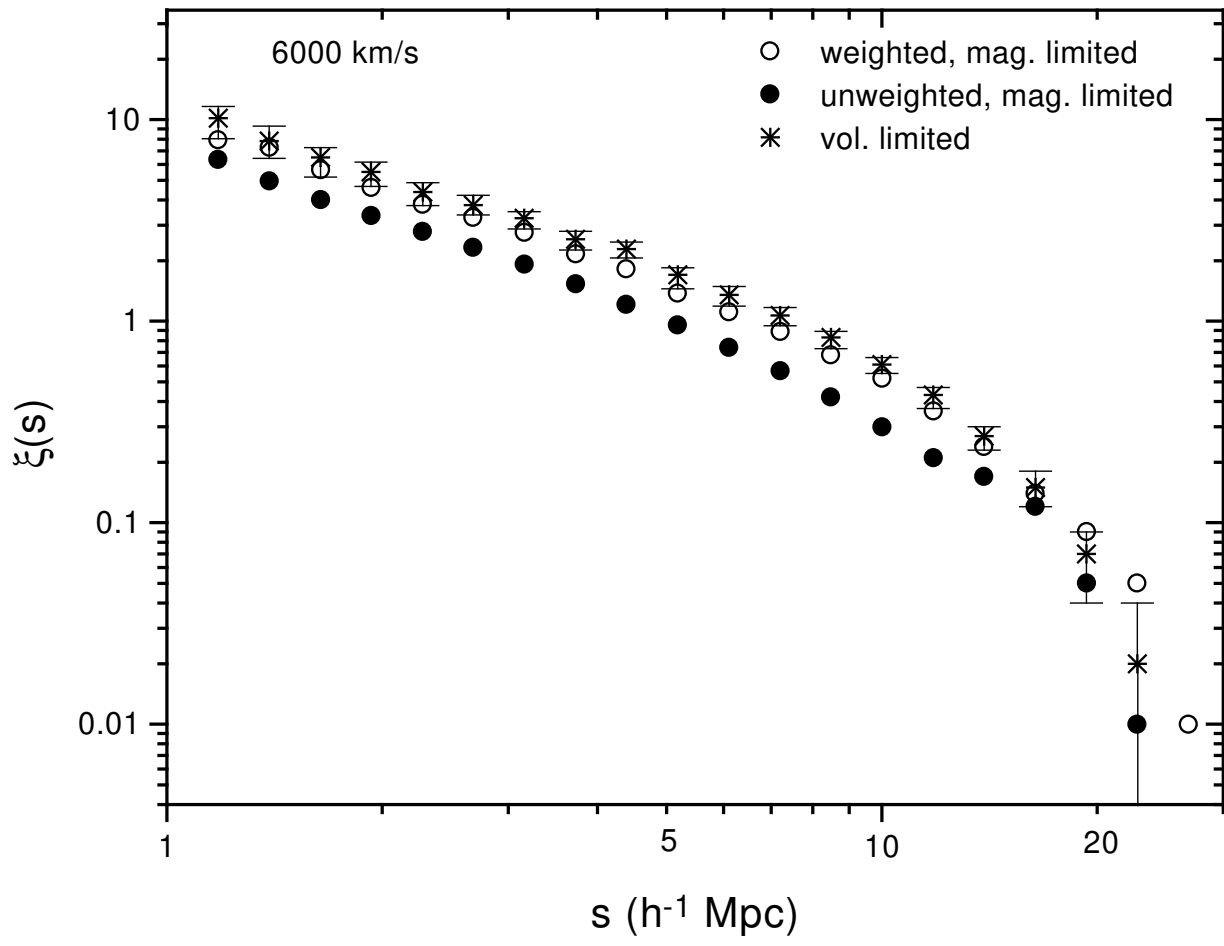
sample	R^y ($h^{-1}Mpc$)	N	(s)
P groups (n 3, low R_{pv})	0.54	71	$0.49^{+0.25}_{-0.26}$
P groups (n 3, high R_{pv})	"	70	$0.64^{+0.41}_{-0.35}$
P groups (n 4, low R_{pv})	0.56	42	$0.56^{+0.32}_{-0.36}$
P groups (n 4, high R_{pv})	"	41	$1.44^{+0.56}_{-0.61}$
P groups (n 4, low R_{pv})	0.70	50	$0.66^{+0.36}_{-0.41}$
P groups (n 4, high R_{pv})	"	33	$1.70^{+0.70}_{-0.75}$
H groups (n 3, low R_{pv})	0.66	70	$0.35^{+0.19}_{-0.20}$
H groups (n 3, high R_{pv})	"	70	$0.77^{+0.31}_{-0.31}$
H groups (n 4, low R_{pv})	0.64	39	$0.45^{+0.27}_{-0.31}$
H groups (n 4, high R_{pv})	"	39	$1.95^{+0.61}_{-0.72}$
H groups (n 4, low R_{pv})	0.90	58	$0.61^{+0.33}_{-0.31}$
H groups (n 4, high R_{pv})	"	20	$3.73^{+1.27}_{-1.16}$
P groups (n 3, low R_m)	0.49	71	$0.49^{+0.21}_{-0.24}$
P groups (n 3, high R_m)	"	70	$0.76^{+0.27}_{-0.33}$
P groups (n 4, low R_m)	0.60	42	$0.74^{+0.48}_{-0.47}$
P groups (n 4, high R_m)	"	41	$1.62^{+0.68}_{-0.73}$
P groups (n 4, low R_m)	0.76	55	$0.65^{+0.66}_{-0.63}$
P groups (n 4, high R_m)	"	28	$1.27^{+0.66}_{-0.63}$
H groups (n 3, low R_m)	0.74	71	$0.46^{+0.26}_{-0.25}$
H groups (n 3, high R_m)	"	70	$1.00^{+0.35}_{-0.33}$
H groups (n 4, low R_m)	0.78	39	$0.89^{+0.52}_{-0.53}$
H groups (n 4, high R_m)	"	39	$1.46^{+0.60}_{-0.59}$
H groups (n 4, low R_m)	1.0	55	$0.83^{+0.39}_{-0.39}$
H groups (n 4, high R_m)	"	23	$2.39^{+1.11}_{-1.05}$

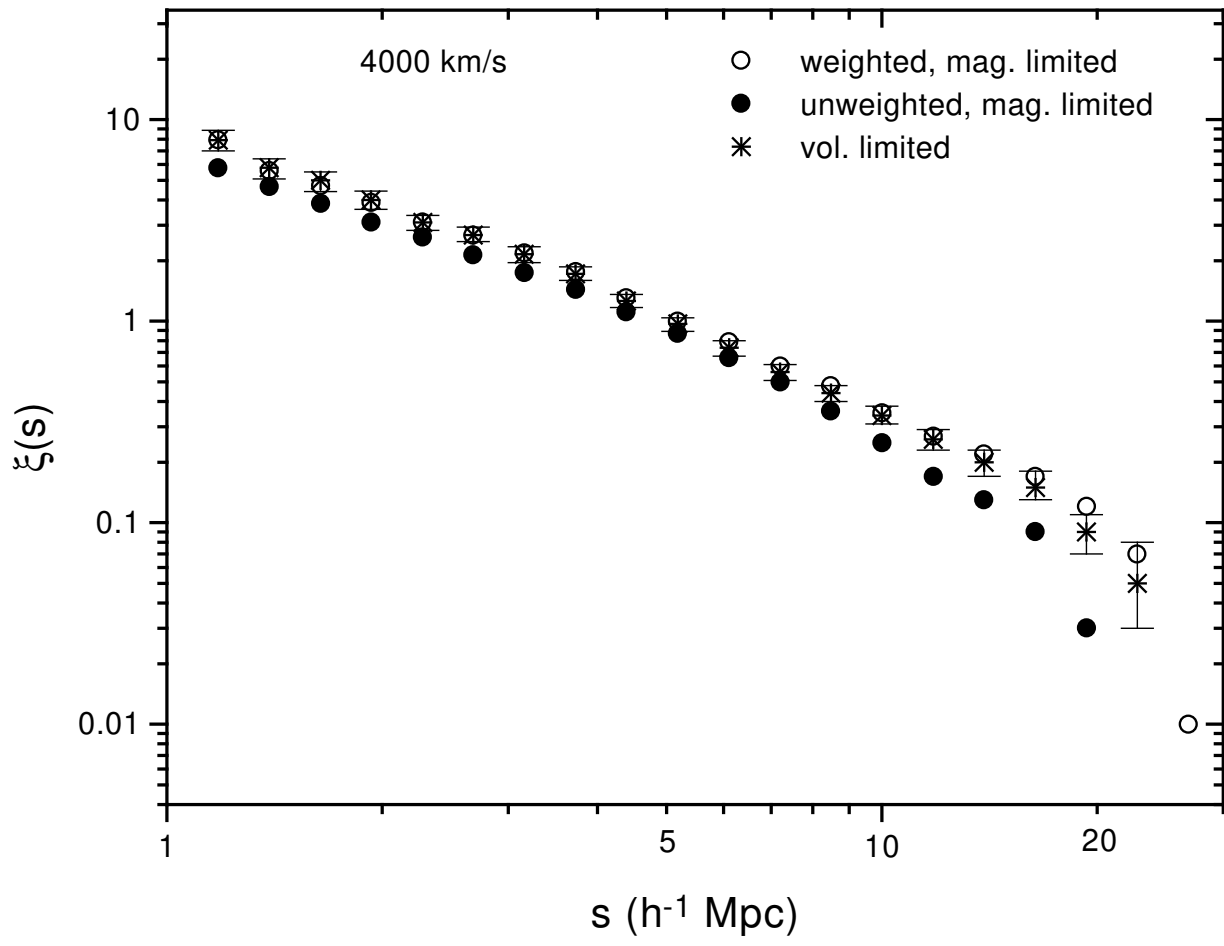
Table 8. Correlation function amplitudes for high- and low-mass groups

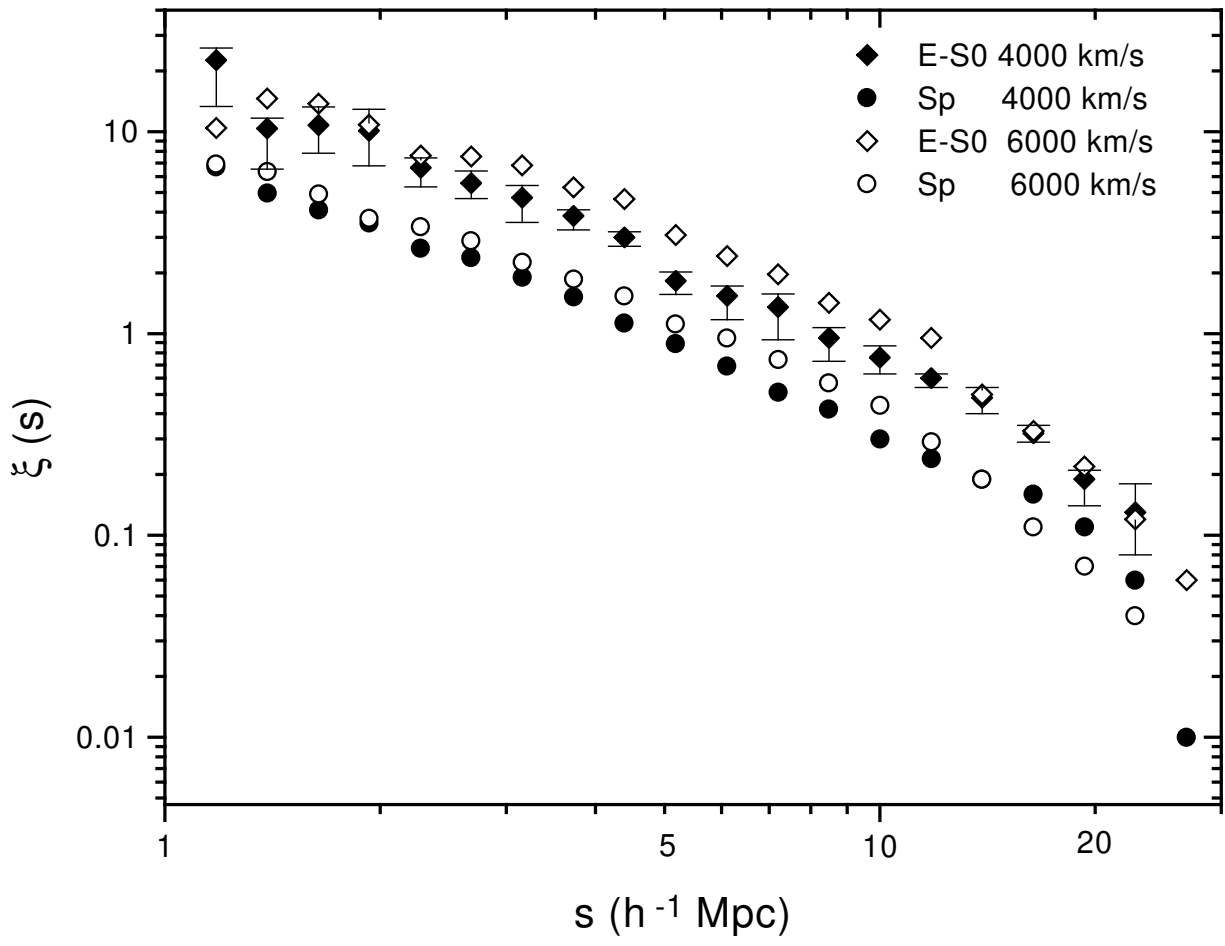
sample	M_{ν}^y ($h^{-1} M_{\odot}$)	N	(s)
P groups (n = 3, low M_{ν})	1:17 10^3	68	$0.58^{+0.28}_{-0.28}$
P groups (n = 3, high M_{ν})	"	67	$0.65^{+0.28}_{-0.30}$
P groups (n = 4, low M_{ν})	1:41 10^3	41	$0.65^{+0.47}_{-0.50}$
P groups (n = 4, high M_{ν})	"	41	$1.17^{+0.46}_{-0.50}$
P groups (n = 4, low M_{ν})	2:70 10^3	55	$0.77^{+0.38}_{-0.38}$
P groups (n = 4, high M_{ν})	"	27	$1.22^{+0.57}_{-0.64}$
H groups (n = 3, low M_{ν})	6:86 10^2	71	$0.40^{+0.28}_{-0.25}$
H groups (n = 3, high M_{ν})	"	69	$1.26^{+0.39}_{-0.39}$
H groups (n = 4, low M_{ν})	9:20 10^2	38	$0.43^{+0.30}_{-0.38}$
H groups (n = 4, high M_{ν})	"	38	$2.60^{+0.76}_{-0.78}$
H groups (n = 4, low M_{ν})	1:5 10^3	49	$0.46^{+0.27}_{-0.23}$
H groups (n = 4, high M_{ν})	"	27	$2.68^{+0.95}_{-0.93}$

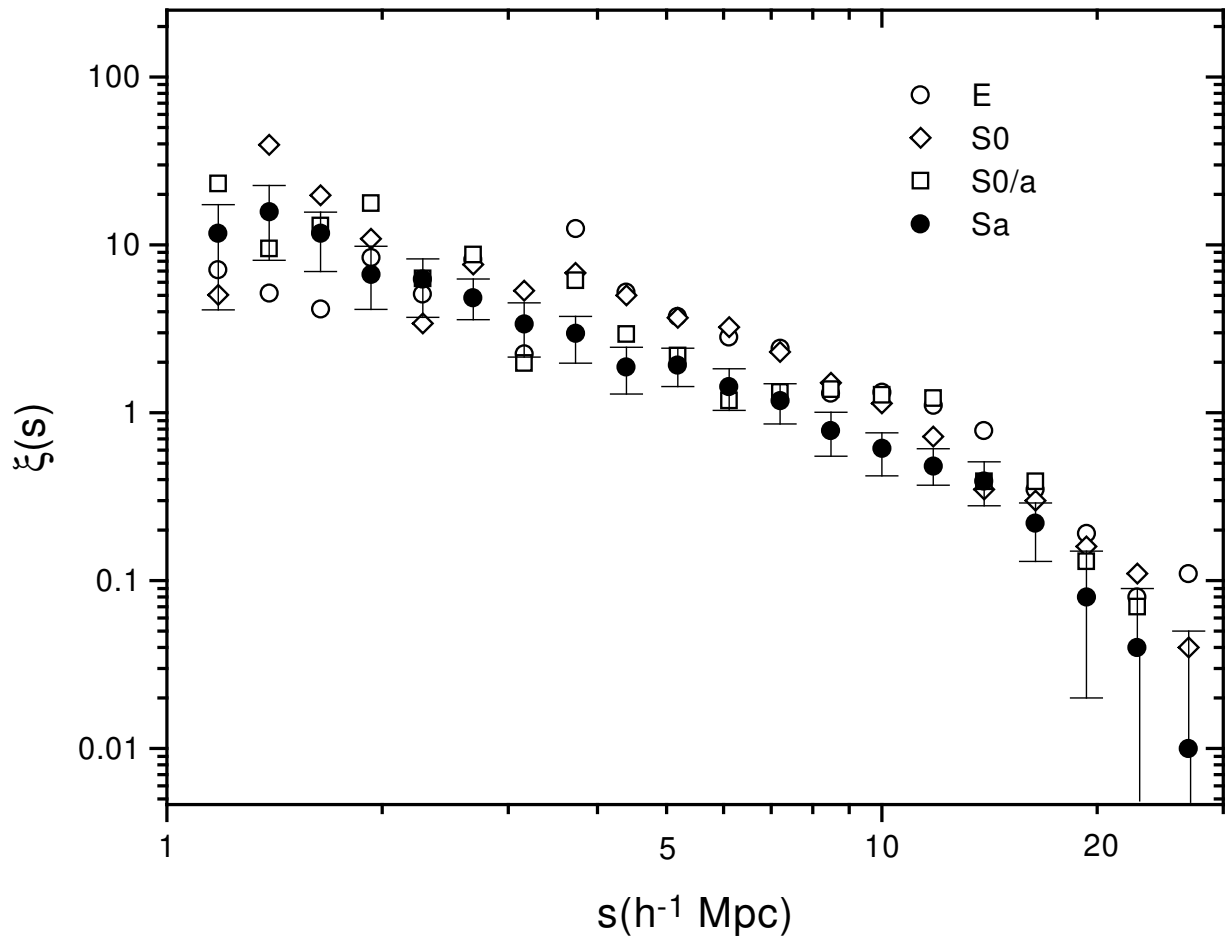
Note. | We denote by M_{ν}^y the limiting value adopted for subdividing each sample of groups into two subsamples of high and low M_{ν} .

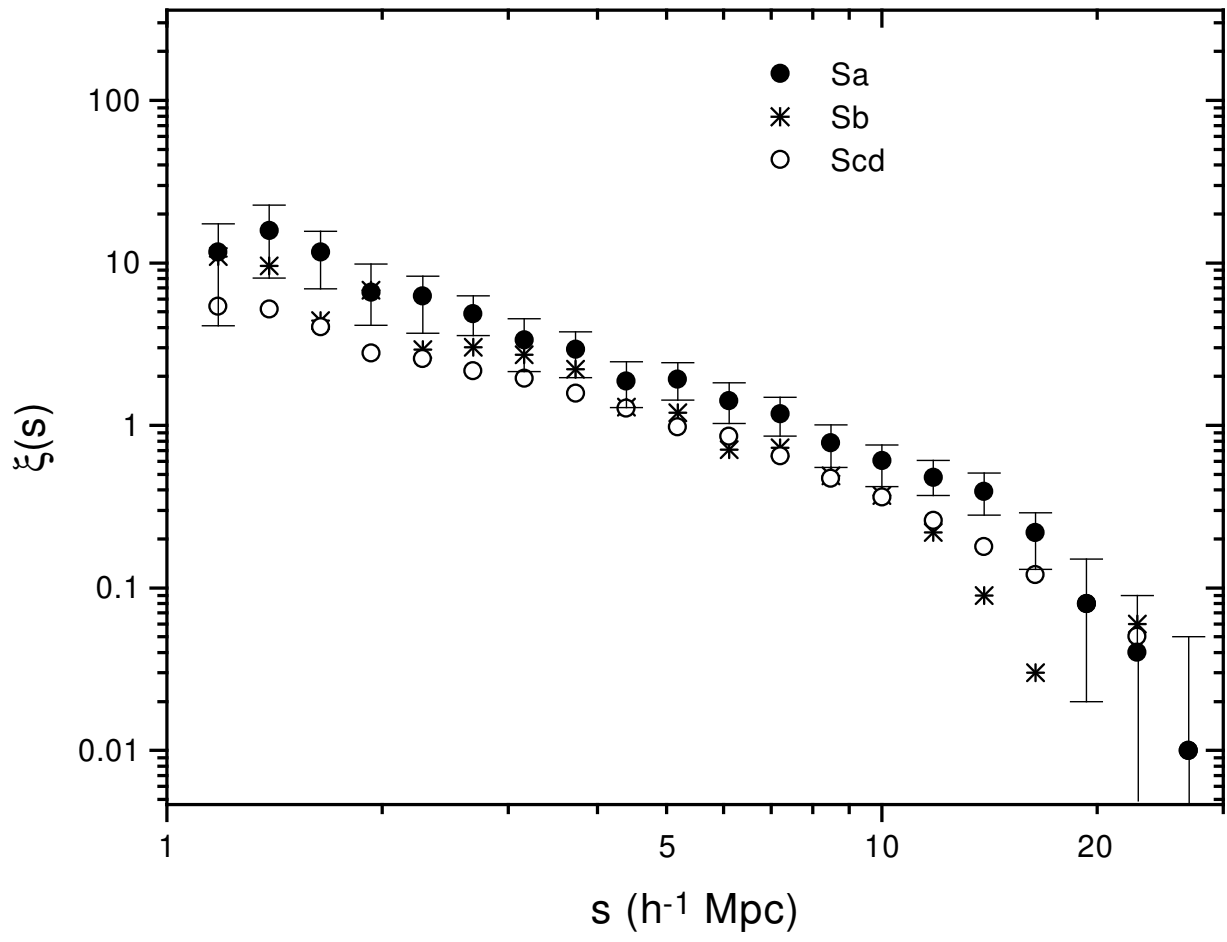


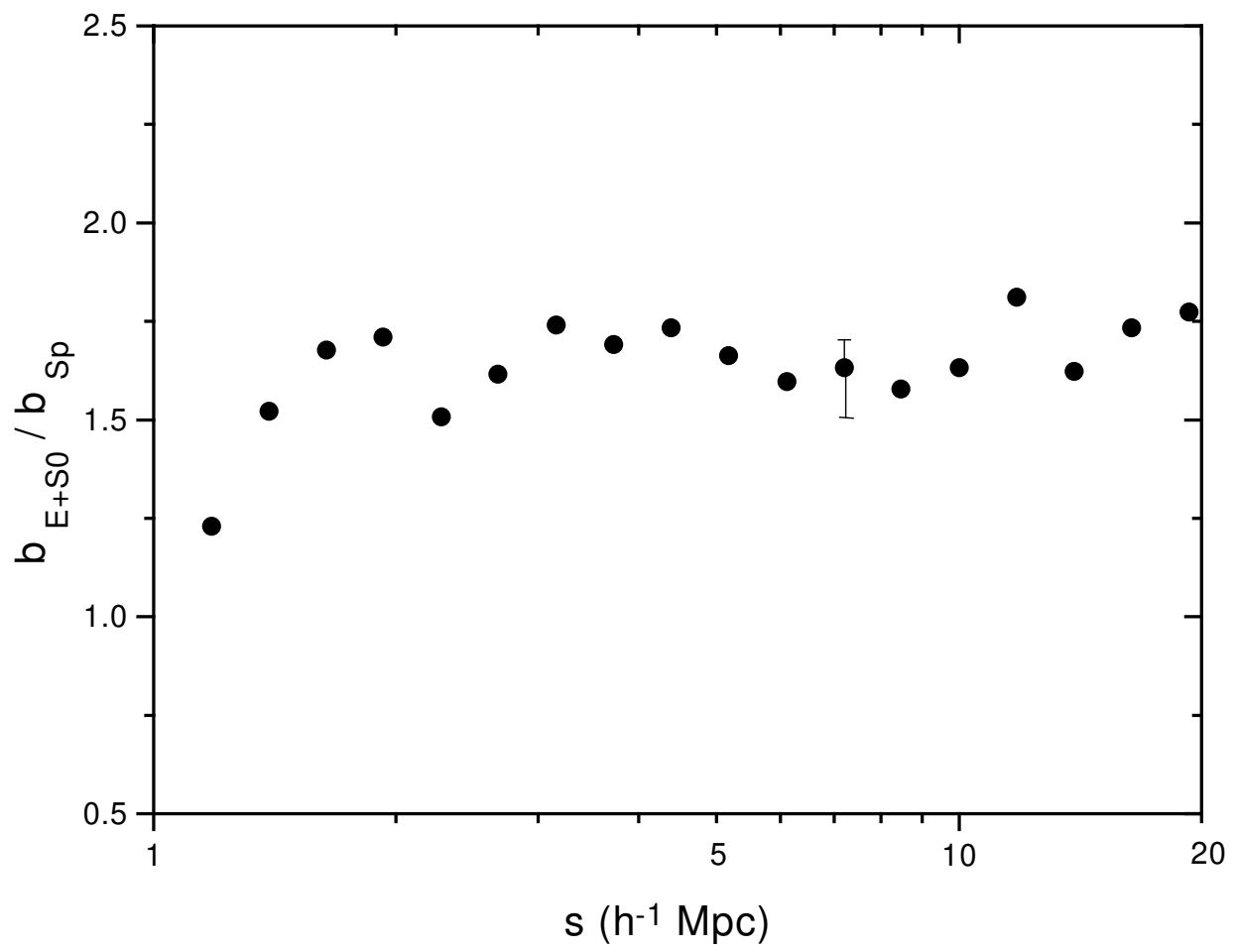


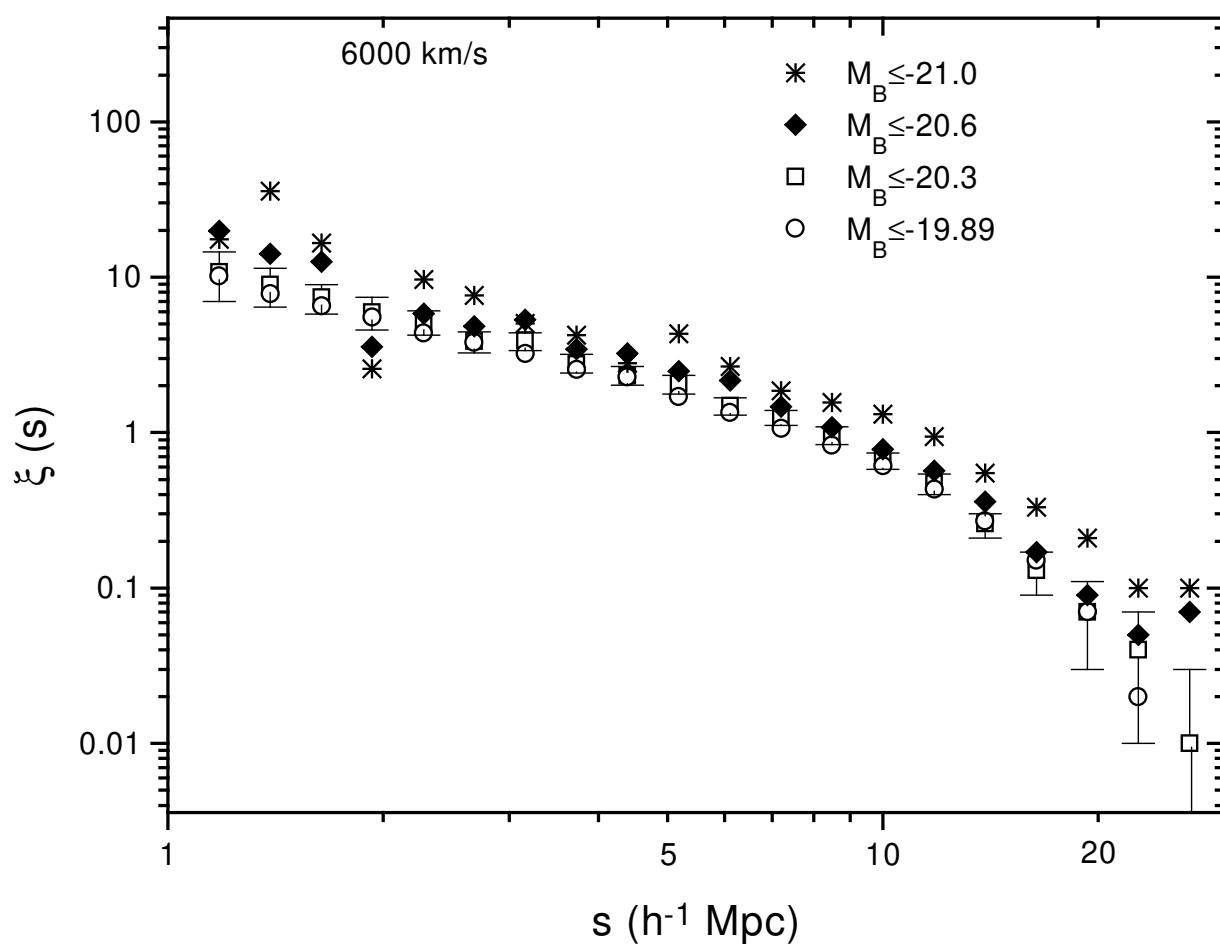


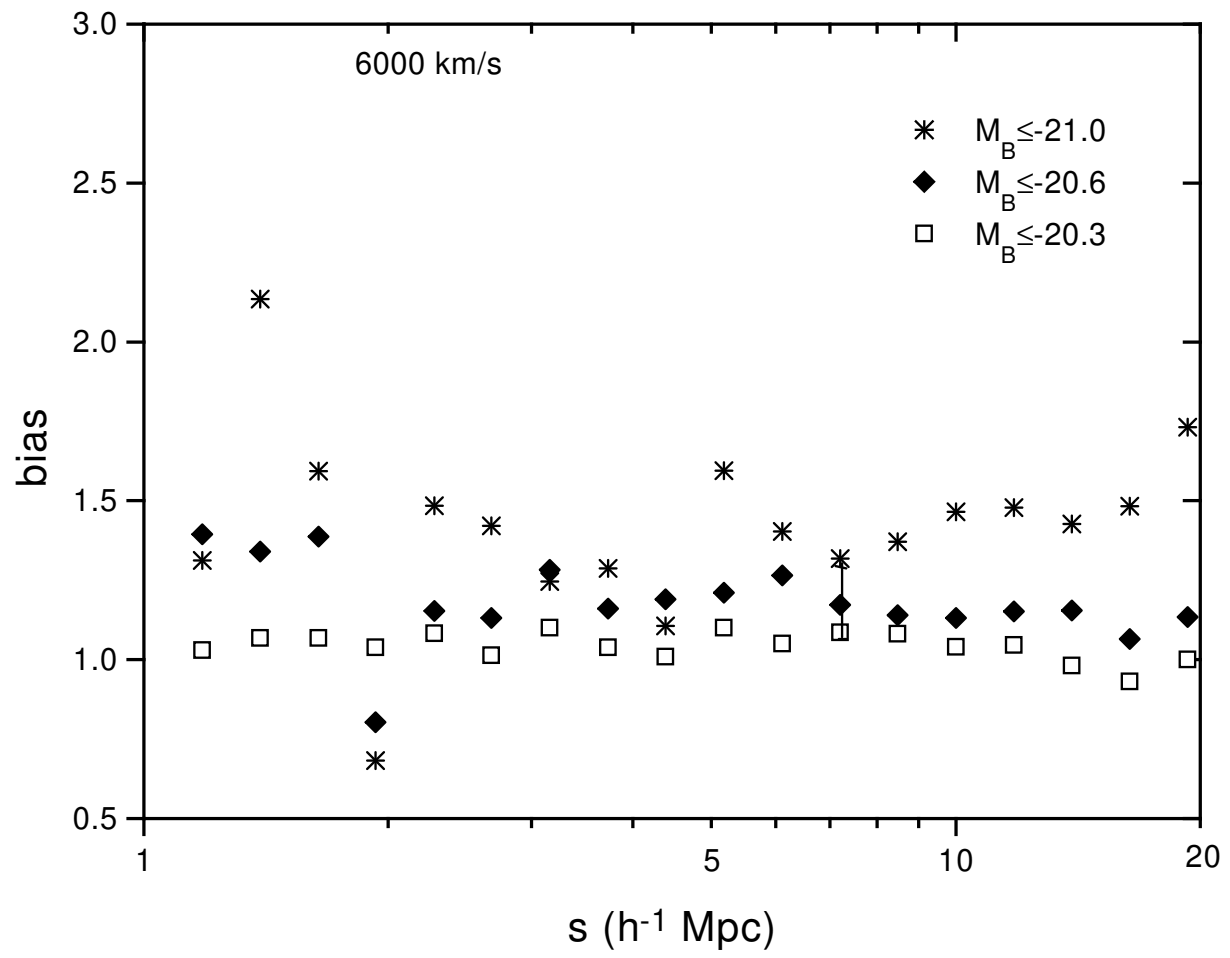


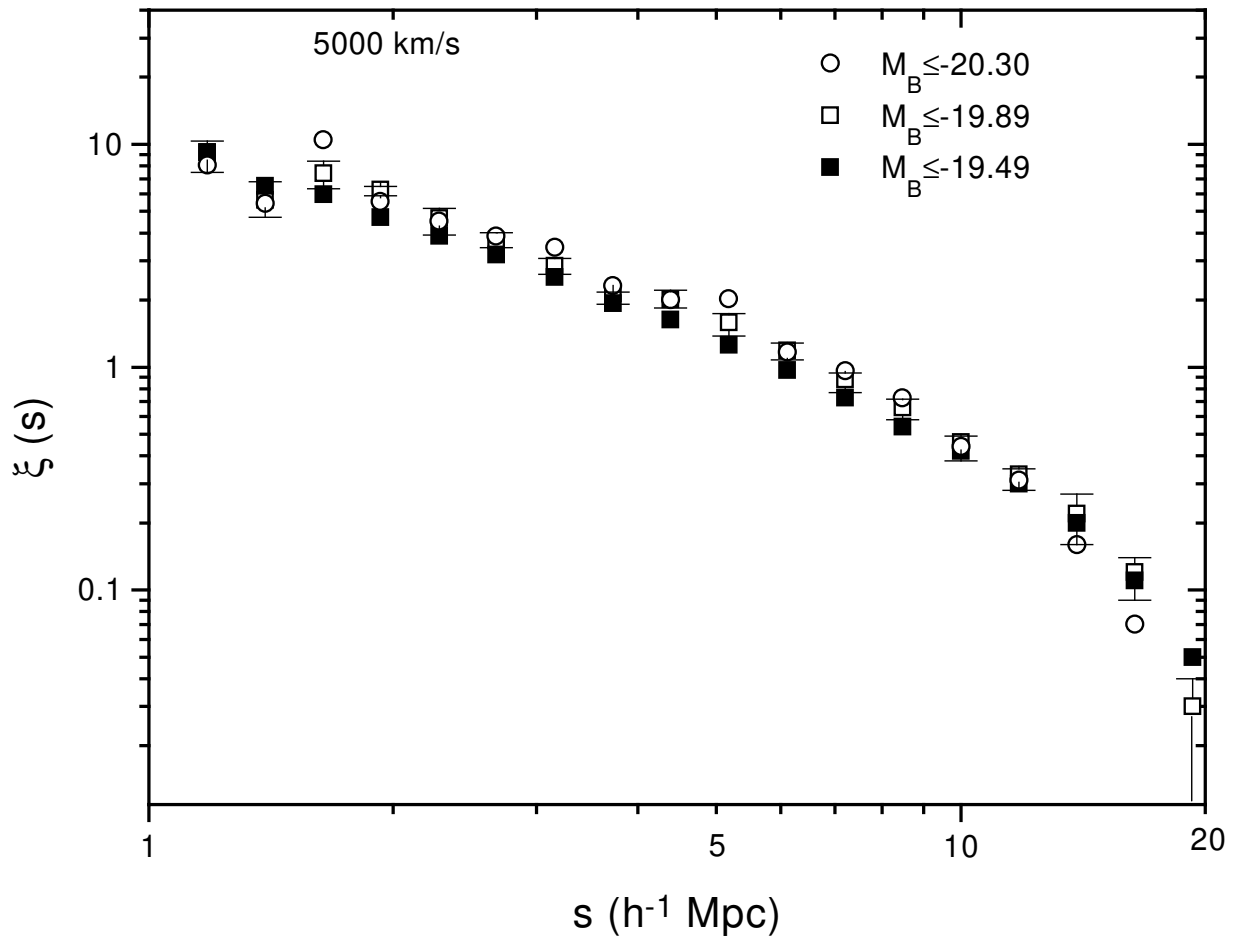


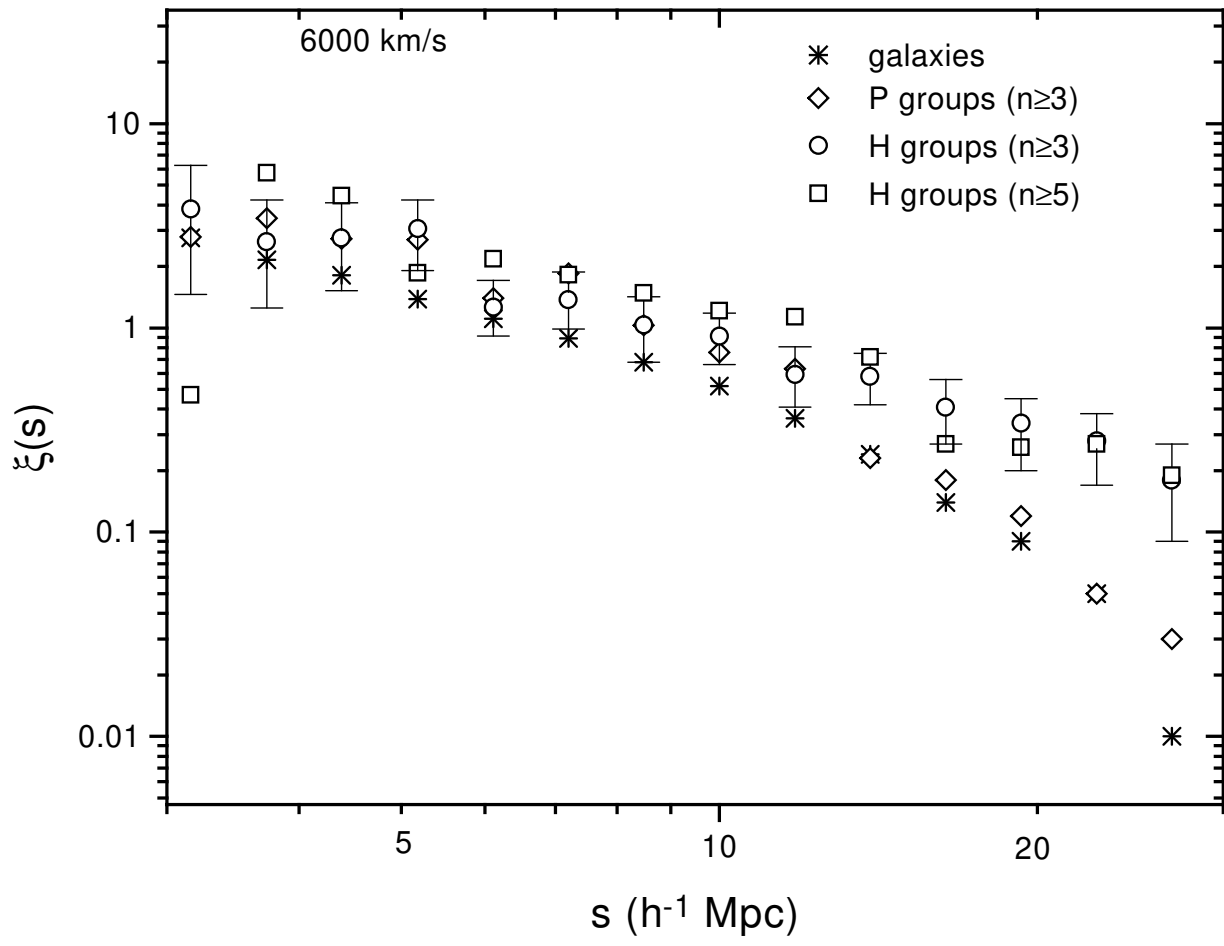


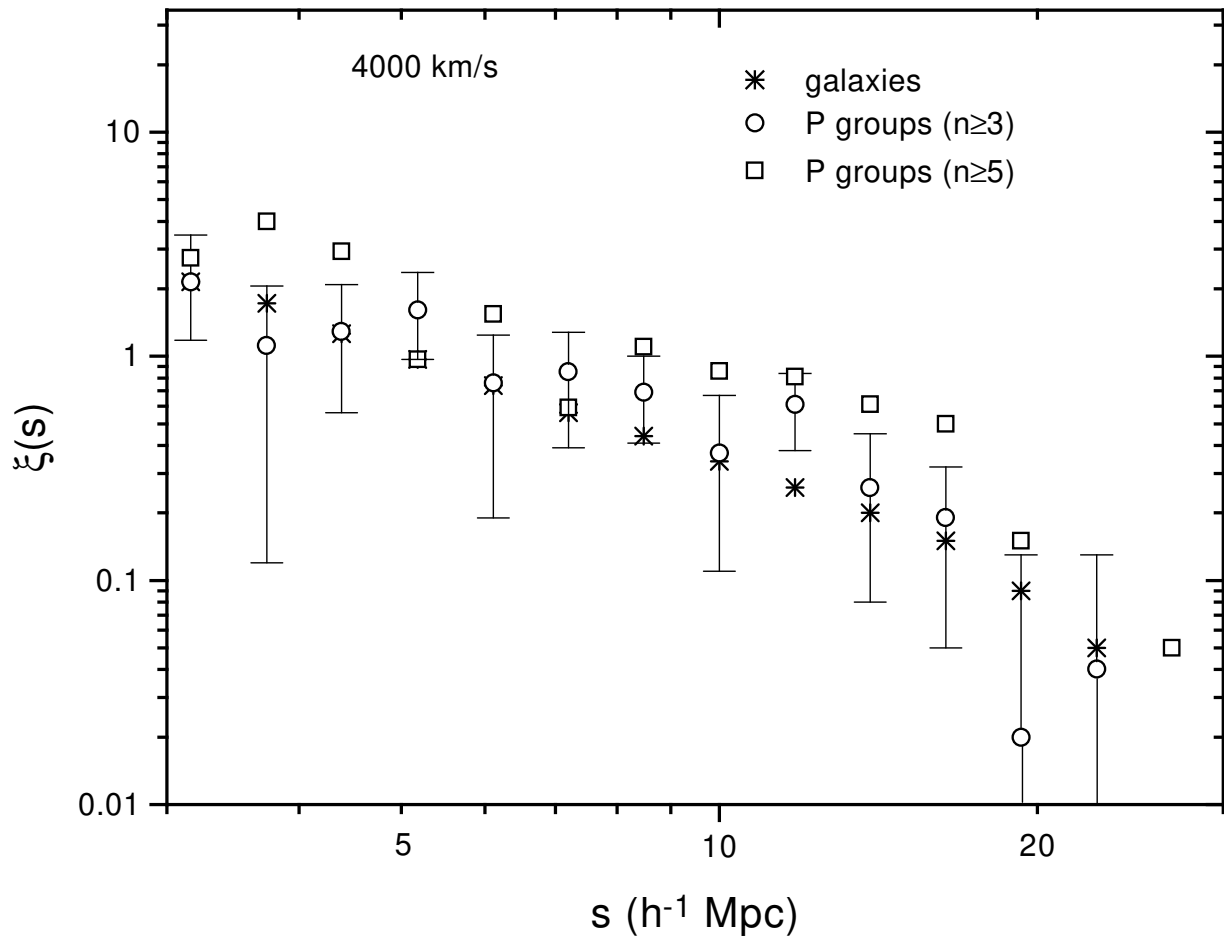


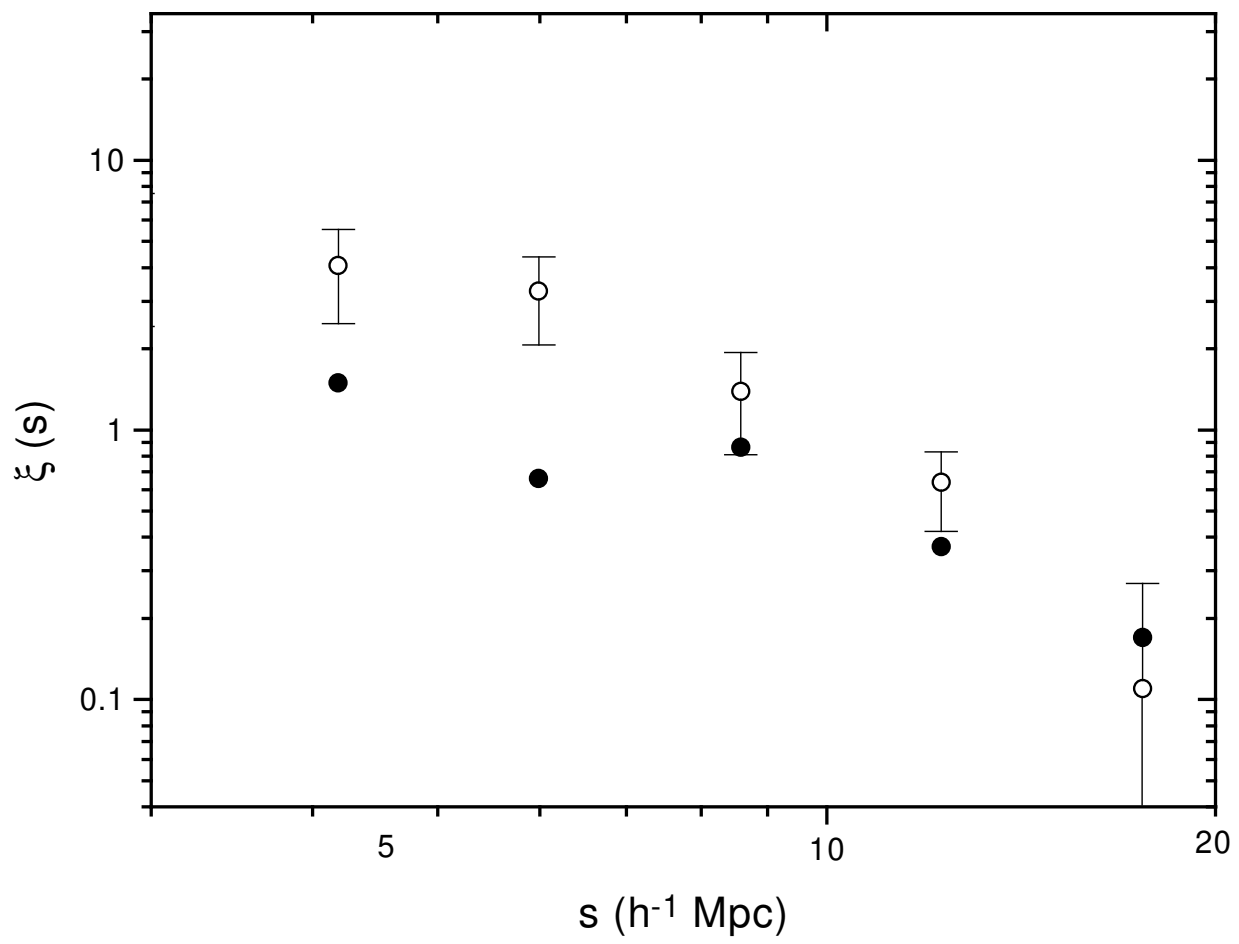












{ 70 {

